Supporting Information

Molecular Dynamics Simulations of Mismatched DNA Duplexes Associated with the Major C^8-Linked 2′-Deoxyguanosine Adduct of the Food Mutagen Ochratoxin A: Influence Of Opposing Base, Adduct Ionization State, and Sequence on the Structure of Damaged DNA

Preetleen Kathuria,[1] Purshotam Sharma,[1] Richard A. Manderville[2] and Stacey D. Wetmore[3]*

[1]*Computational Biochemistry Laboratory, Department of Chemistry and Centre for Advanced Studies in Chemistry, Panjab University, Chandigarh, India 160014.* [2]*Departments of Chemistry and Toxicology, University of Guelph, Guelph, Ontario, Canada N1G 2W1.* [3]*Department of Chemistry and Biochemistry, University of Lethbridge, Lethbridge, Alberta, Canada T1K 3M4.*

*E-mail: stacey.wetmore@uleth.ca. Telephone: (403) 329-2323. Fax: (403) 329-2057

Table of Contents

Section S1. Additional details of the computational protocol.

Starting Structures: A 12-mer DNA oligonucleotide (5′−CTCG[1]G[2]CG[3]CCATC) containing the mutagenic *Nar*I recognition sequence (underlined)[1] was used for MD simulations. Specifically, the OT-G adduct in each of four ionization states (i.e., the physiologically relevant COO^-, ArO^- and dianionic states, as well as the neutral (control) state) was reiteratively placed at the G^1, G^2 or G^3 position, and paired opposite A, T or G. Initial conformations were considered in accordance with the three conformational themes (i.e., B, W and S, Figure 1B–D) previously reported for the C^8-bonded aromatic amine adducts,[2] as well as the OT-G adduct paired opposite C.[3, 4] These conformers were studied for all combinations of four OT-G ionization states, three sequence contexts and three mismatched bases, leading to a total of (3*4*3*3) 108 distinct conformers. Trial simulations were carried out with different starting structures, in attempts to ensure final production simulations correspond to each of the three conformational themes and hydrogen bonding at the terminal ends remain intact (Tables S16–S18), thereby allowing meaningful comparison of the free energies. Simulations for which the correct conformation was not obtained or terminal base pairs did not remain intact were discarded and new starting structures were used to re-simulate the associated conformation. New starting structures were obtained either by fine-tuning the initial structure, the representative structure from a previous simulation or the representative structure corresponding to the same conformation with a different adduct ionization state. However, the S conformer of G mismatched DNA

containing ArO^- OT-G at G^2 and dianionic OT-G at G^3 could not be isolated, with the structure reverting to the W conformer. Additionally, since our previous study (ref. 19 of manuscript) did not consider the ArO^- ionization state of OT-G, simulations for ArO^- OT-G incorporated at G^1, G^2 and G^3 paired against C were also conducted for comparison.

Simulation Details: Each DNA oligonucleotide was neutralized using 22 sodium ions and solvated in an octahedral box containing TIP3P water[5] using the pmemd module of AMBER 12,[6] such that each DNA atom at least 8 Å away from the edge of the box. The natural and modified DNA nucleotides were described using the parmbsc0 modification[7] of parm99,[8] and additional parameters and partial charges for the OT-G nucleotide were taken from our previous studies (Tables S19–S22).[3, 4] While applying a 500 kcal $mol^{-1}Å^{-2}$ restraint on DNA, the ions and water molecules within the box were initially minimized using 500 steps of steepest decent (SD), and 500 steps of conjugate gradient (CG), minimization. Subsequently, the restraint on DNA was removed and the whole system was minimized using 1000 steps of SD, and 1500 steps of CG, minimization. The temperature of the system was then increased from 0 to 300 K by employing a Langevin temperature equilibration scheme, and the system was simulated for 20 ps at constant volume. A cut-off of 10 Å for the non-bonded interactions was used in our simulations. To analyze the effect of changing the non-bonded cut-off, we repeated a set of simulations with a box length of 10 Å and a non-bonded cut-off of 9 Å. The structural parameters derived from these simulations match those from our original simulations (Figure 26, and Tables S23–S24). Finally, a total of 108 production MD simulations of 40 ns duration were carried out using an NPT ensemble with a Brendsen barostat.

To ensure key DNA structural parameters are converged and obtain the most reliable conclusions, all simulation frames between 30 and 40 ns were used for the detailed structural and free energy analyses. A similar protocol has previously been used in MD studies of natural[9] and damaged[9-11] DNA. For each system, no significant fluctuations were observed in the backbone rmsd over the last 10 ns calculated with respect to the first frame of the production simulation (Figures S23-S25). To further ensure convergence of key structural parameters, a set of simulations were extended for 500 ns, which lead to similar structural and energetic parameters as the original simulations (Figure S27, and Tables S25–S26).

Representative structures for each adducted DNA conformer were obtained by clustering the final 10 ns of the simulation with respect to the χ and θ dihedral angles (Figure 1A). Additionally, the lesion site van der Waals stacking energies between the OT-G adduct or the partner base (A, G or T) and the 3′ or 5′–flanking base pairs were calculated for the B and W adducted DNA conformers. For the S conformer, the opposing base was excluded

from this analysis since it is displaced out of the helix and does not significantly contribute to the stacking energy. The interaction energies between the hydrogen-bonded base pairs were approximated as the electrostatic interaction energy between the nucleobase atoms of the base pairs, whereas the stacking energies were approximated as the van der Waals interaction energy between the nucleobase atoms of the stacked bases. These energies were calculated using the LIE command in AMBERTOOLS. All these analyses were done using cpptraj module of AMBER 12.[6]

Free energy analysis: The MM-PBSA[12] free energy (G) for each system was calculated as the sum of the solvation energy (E^{sol}), molecular mechanics energy (E^{MM}) and the entropy term (TS). Thus,

$$G = E^{MM} + E^{sol} - TS$$

where T is the temperature and S is the sum of rotational, translational and vibrational entropies for the DNA using the MMPBSA method. The E^{MM} term was estimated by summing the internal energy (E^{int}), which contains sum of bonded energy terms such as energy for the bonds (E^{bonds}), bond angles (E^{angles}) and dihedral angles ($E^{dihedrals}$), and the non-bonded contributions including the van der Waals energy (E^{vdW}) and electrostatic energy (E^{elec}). The solvation term (E^{sol}) was estimated as the sum of polar and non-polar contributions where the polar contribution is estimated using the Poisson-Boltzmann method. In accordance with previous studies on damaged DNA,[4, 13] 1000 frames (i.e., 1 snapshot every 5 ps) were used to calculate the enthalpy and solvation terms, while 100 frames (i.e., 1 snapshot every 50 ps) were used to calculate the entropy term. The energy for each system is calculated and reported relative to the most stable conformer with the similar ionization state, sequence context and the mismatched base. The MM-PBSA (molecular mechanics-Poisson Boltzmann surface area) method was employed to estimate the relative free energies of the adducted DNA conformers.

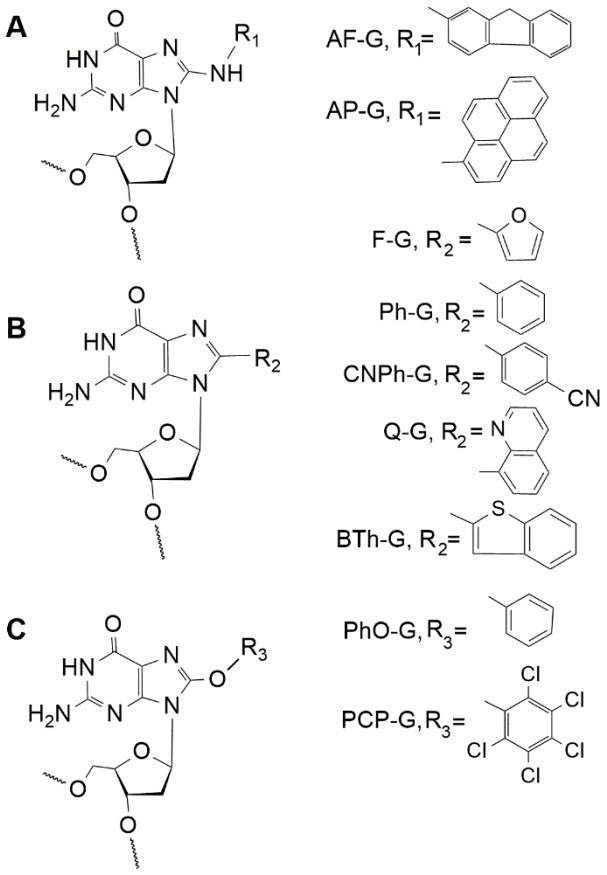

Figure S1. Structures of (**A**) N-linked, (**B**) C-linked and (**C**) O-linked C^8-G nucleoside adducts previously studied in mismatched DNA duplexes.

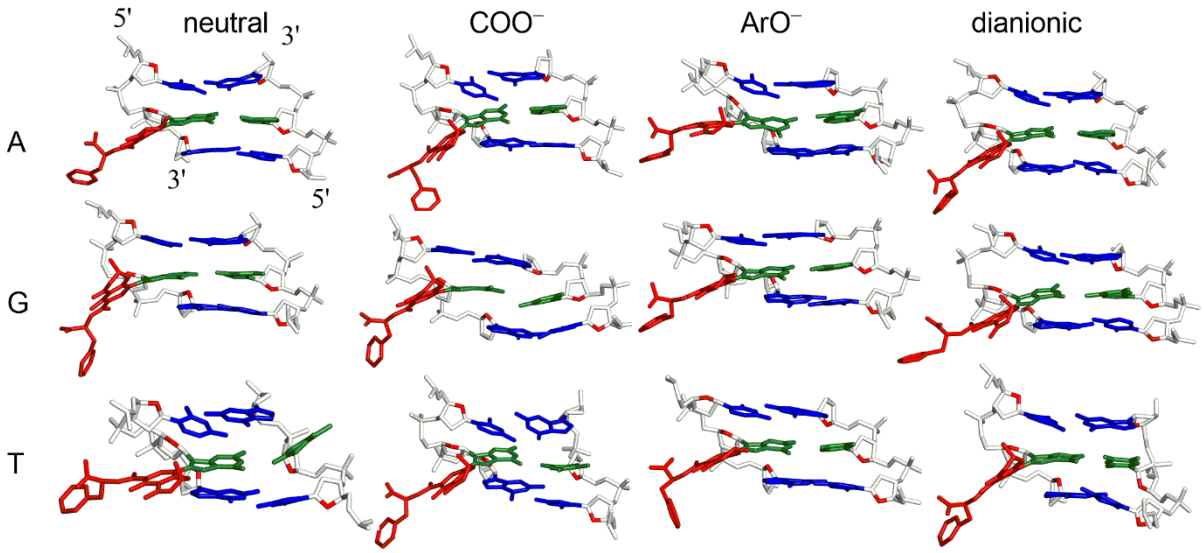

Figure S2. Representative lesion-site structures of the major groove (B) conformers of DNA containing OT-G in different ionization states at the G^1 position and paired opposite A, G or T. The OT moiety is shown in red, the damaged G moiety and the opposing base in green, and the base pairs flanking the lesion in blue.

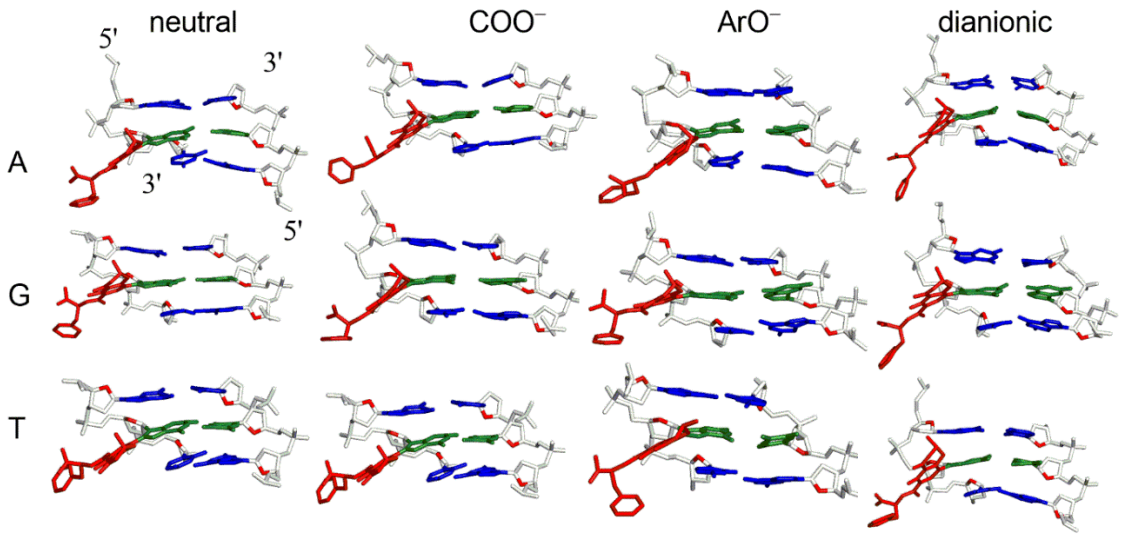

Figure S3. Representative lesion-site structures of the major groove (B) conformers of DNA containing OT-G in different ionization states at the G^2 position and paired opposite A, G or T. The OT moiety is shown in red, the damaged G moiety and the opposing base in green, and the base pairs flanking the lesion in blue.

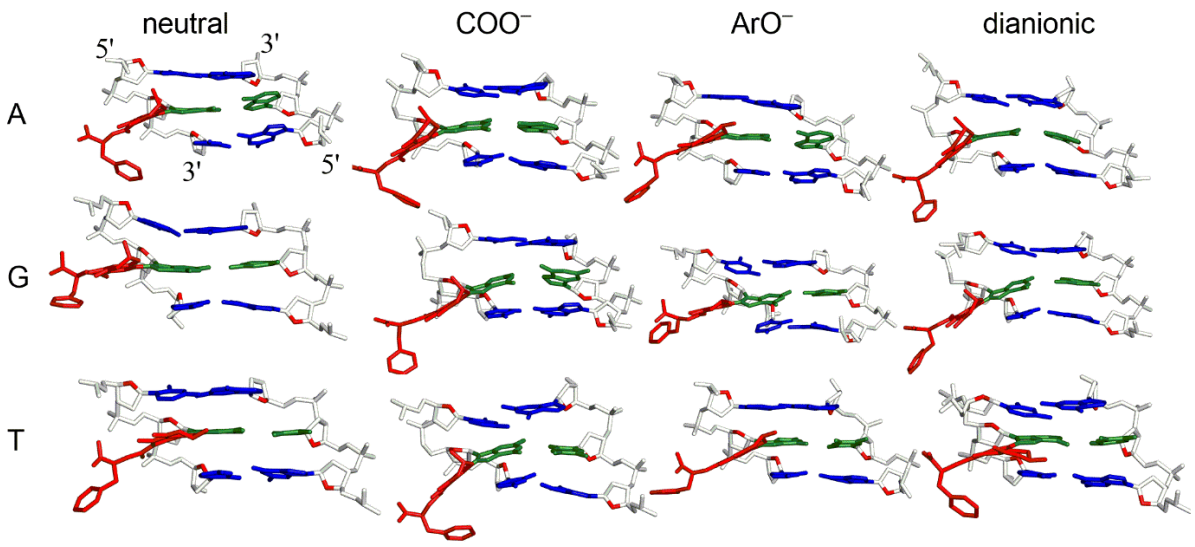

Figure S4. Representative lesion-site structures of the major groove (B) conformers of DNA containing OT-G in different ionization states at the G^3 position and paired opposite A, G or T. The OT moiety is shown in red, the damaged G moiety and the opposing base in green, and the base pairs flanking the lesion in blue.

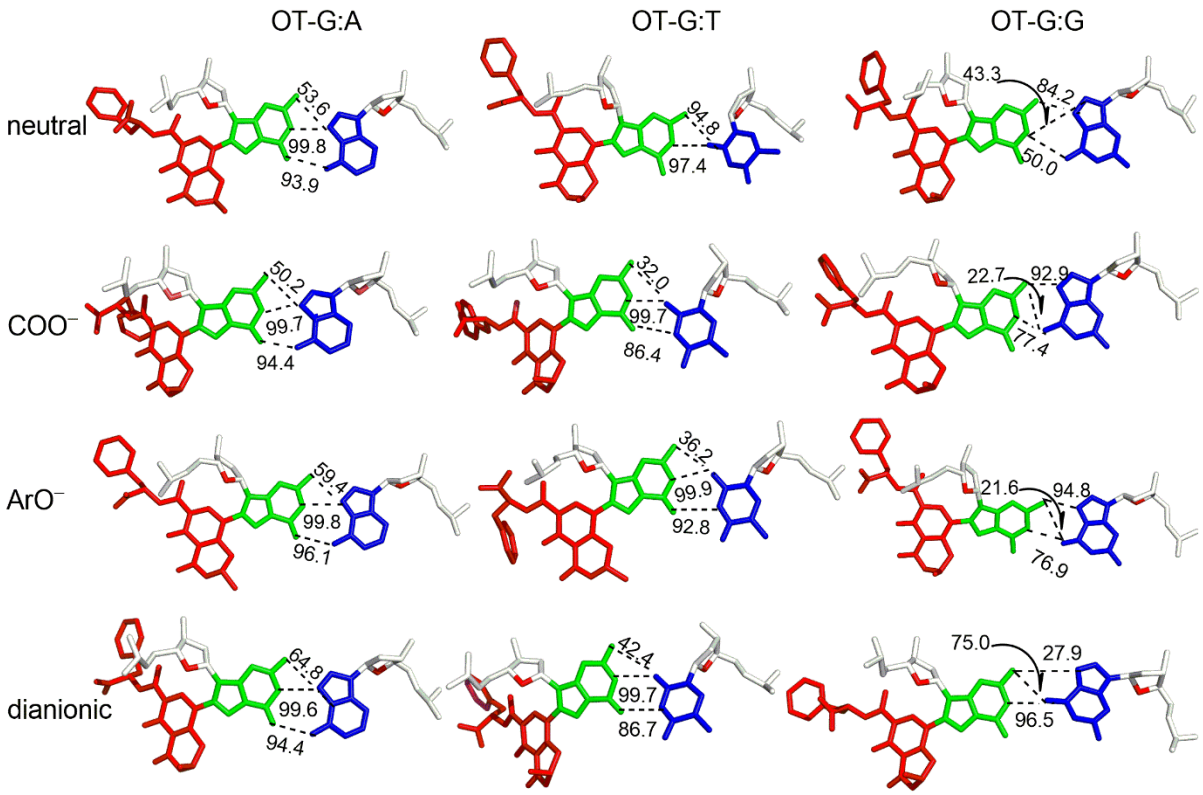

Figure S5. Lesion-site hydrogen bonding for OT-G in different ionization states at the G^1 position mispaired against A, T or G in the B adducted DNA conformation.

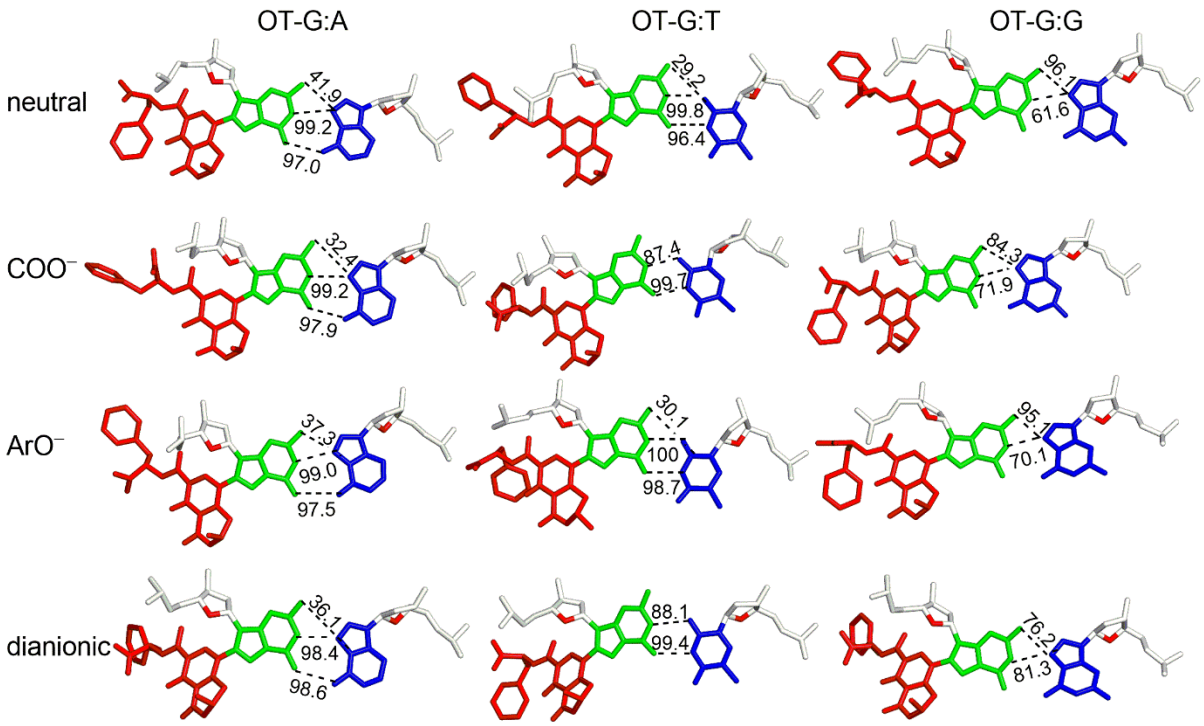

Figure S6. Lesion-site hydrogen bonding for OT-G in different ionization states at the G^2 position mispaired against A, T or G in the B adducted DNA conformation.

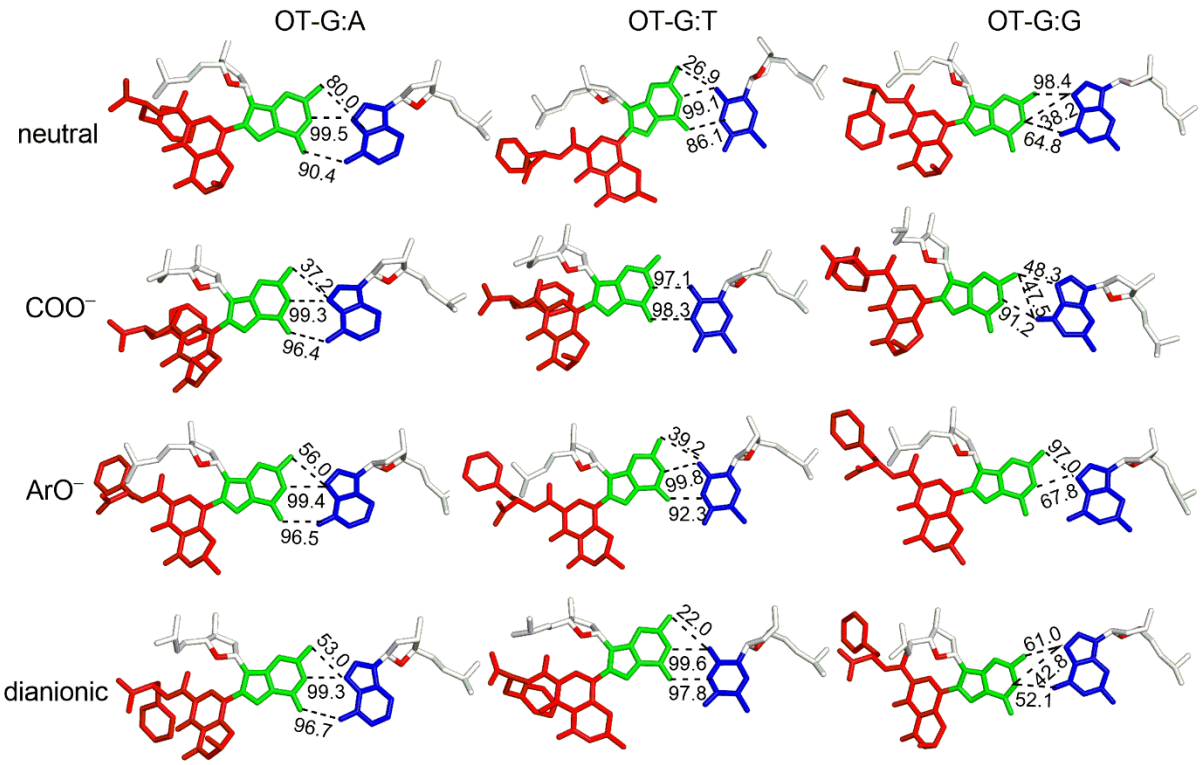

Figure S7. Lesion-site hydrogen bonding for OT-G in different ionization states at the G^3 position mispaired against A, T or G in the B adducted DNA conformation.

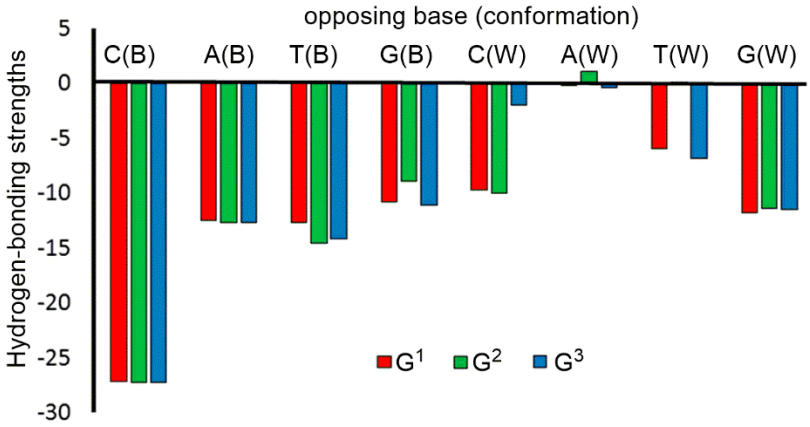

Figure S8. Hydrogen-bonding energies (kcal mol^{-1}) between neutral OT-G and the opposing base in the B and W adducted DNA conformations for three sequence contexts. Data for C match is taken from reference 19 of the manuscript.

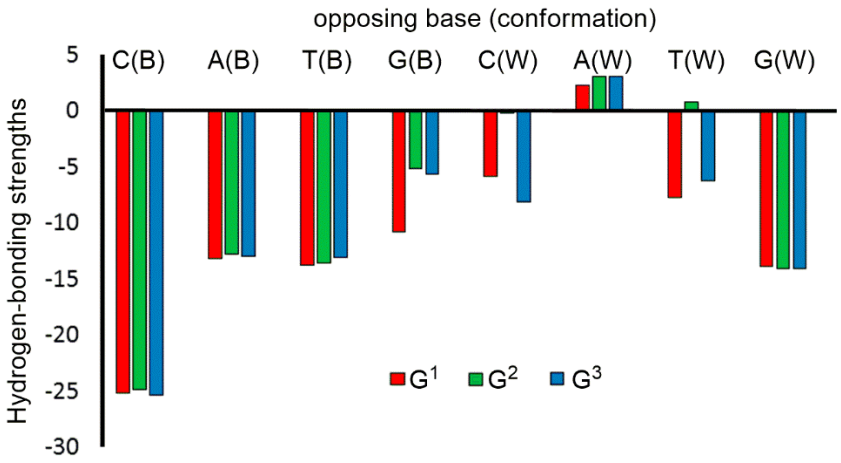

Figure S9. Hydrogen-bonding energies (kcal mol^{-1}) between the ArO^- OT-G and the opposing base in the B and W adducted DNA conformations for three sequence contexts.

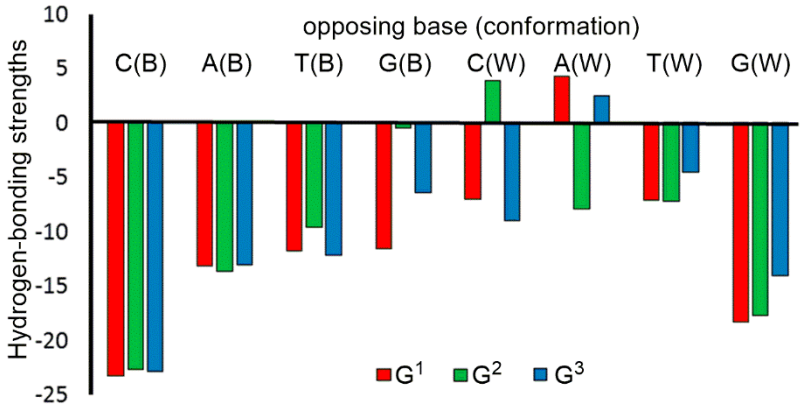

Figure S10. Hydrogen-bonding energies (kcal mol^{-1}) between dianioinic OT-G and the opposing base in the B and W adducted DNA conformations for three sequence contexts. Data for C match is taken from reference 19 of the manuscript.

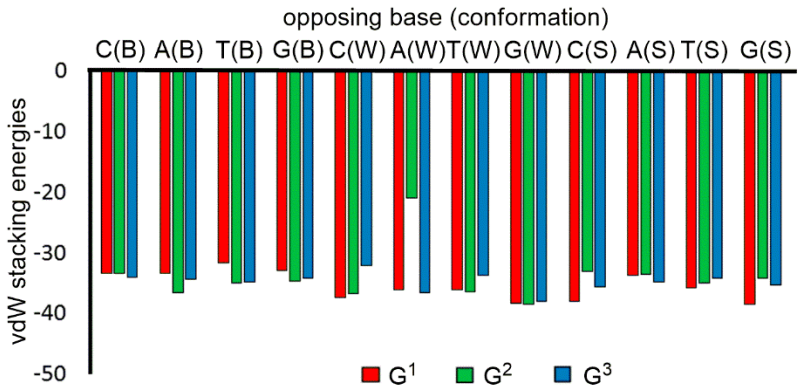

Figure S11. van der Waals (vdW) stacking energies (kcal mol^{-1}) of neutral OT-G and the opposing base with the flanking base pairs (for the B and W conformers), and neutral OT-G with the flanking base pairs (for the S conformer) for different opposing bases and sequence contexts. Data for C match is taken from reference 19 of the manuscript.

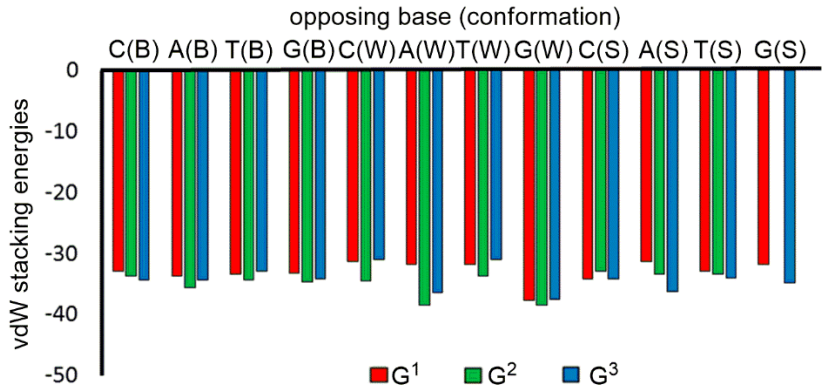

Figure S12. van der Waals (vdW) stacking energies (kcal mol^{-1}) of ArO^- OT-G and the opposing base with the flanking base pairs (for the B and W conformers), and ArO^- OT-G with the flanking base pairs (for the S conformer) for different opposing bases and sequence contexts. Data for C match is taken from reference 19 of the manuscript.

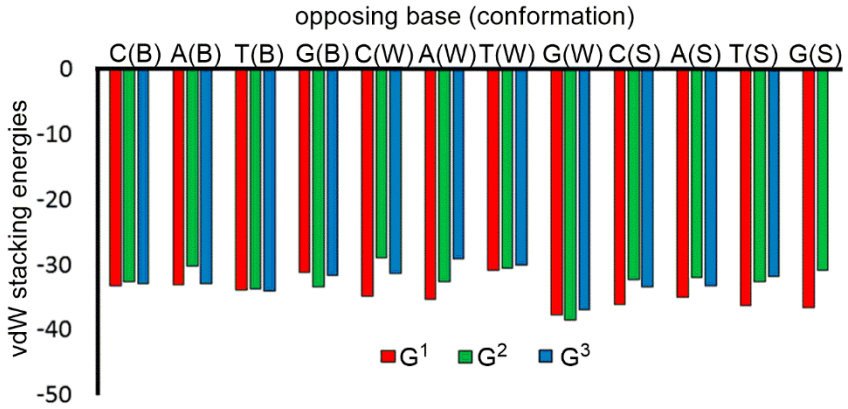

Figure S13. van der Waals (vdW) stacking energies (kcal mol^{-1}) of dianionic OT-G and the opposing base with the flanking base pairs (for the B and W conformers), and dianionic OT-G with the flanking base pairs (for the S conformer) for different opposing bases and sequence contexts. Data for C match is taken from reference 199 of the manuscript.

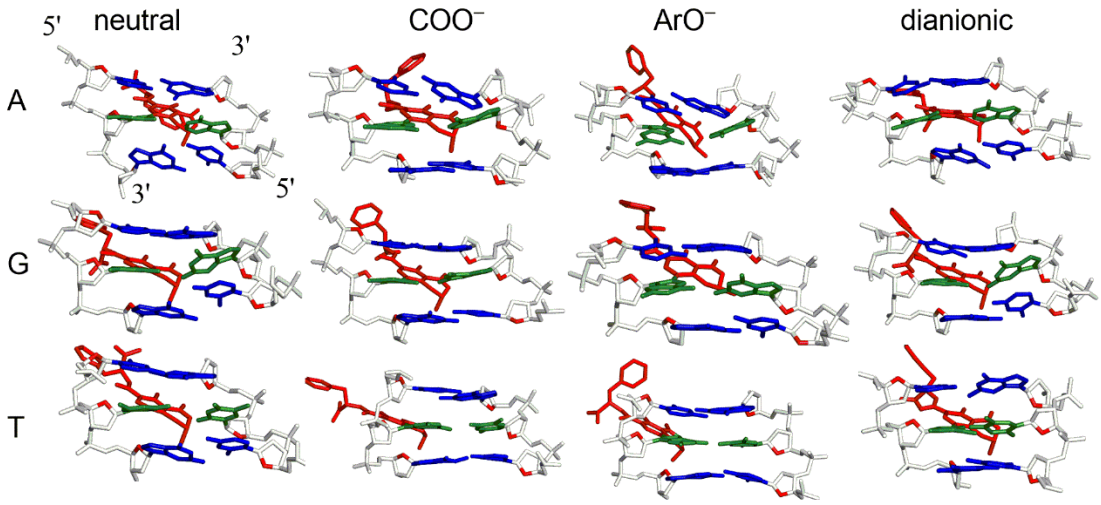

Figure S14. Representative lesion-site structures of the wedge (W) conformers of DNA containing OT-G in different ionization states at the G^1 position and paired opposite A, G or T. The OT moiety is shown in red, the damaged G moiety and the opposing base in green, and the base pairs flanking the lesion in blue.

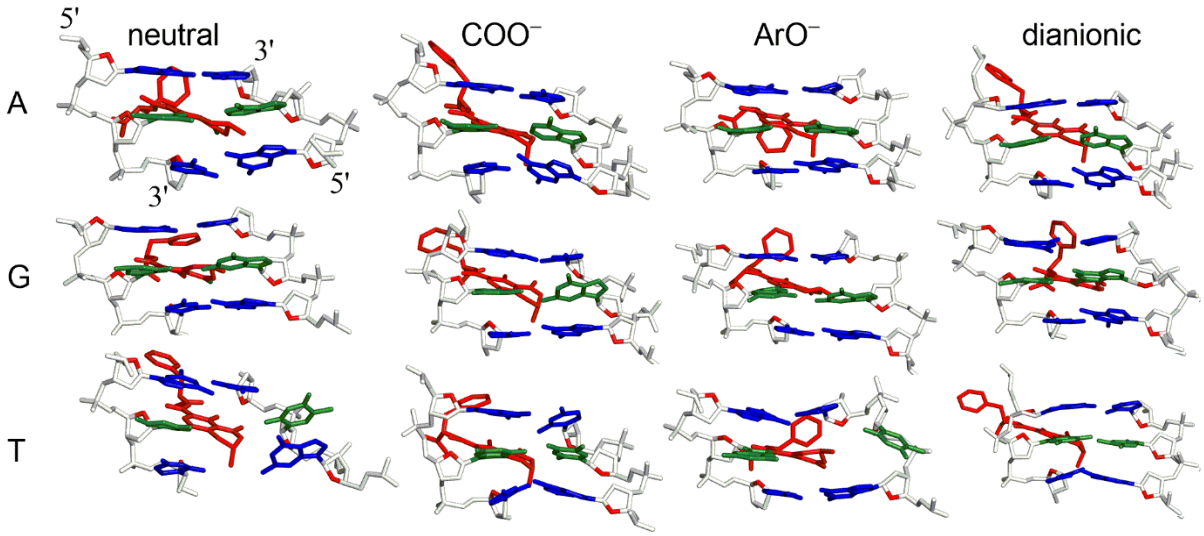

Figure S15. Representative lesion-site structures of the wedge (W) conformers of DNA containing OT-G in different ionization states at the G^2 position and paired opposite A, G or T. The OT moiety is shown in red, the damaged G moiety and the opposing base in green, and the base pairs flanking the lesion in blue.

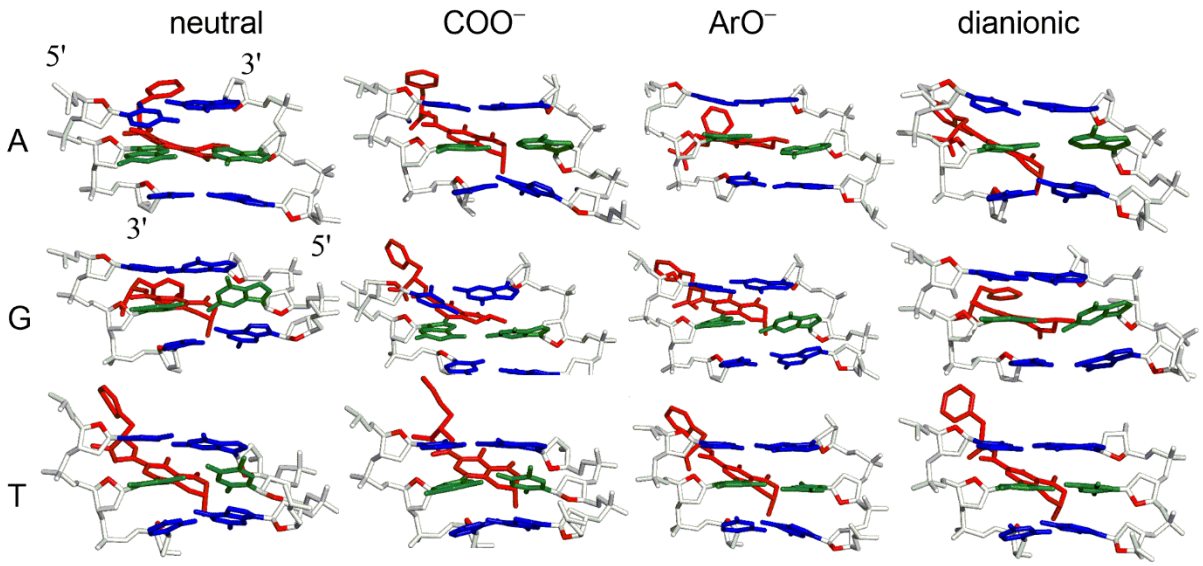

Figure S16. Representative lesion-site structures of the wedge (W) conformers of DNA containing OT-G in different ionization states at the G^3 position and paired opposite A, G or T. The OT moiety is shown in red, the damaged G moiety and the opposing base in green, and the base pairs flanking the lesion in blue.

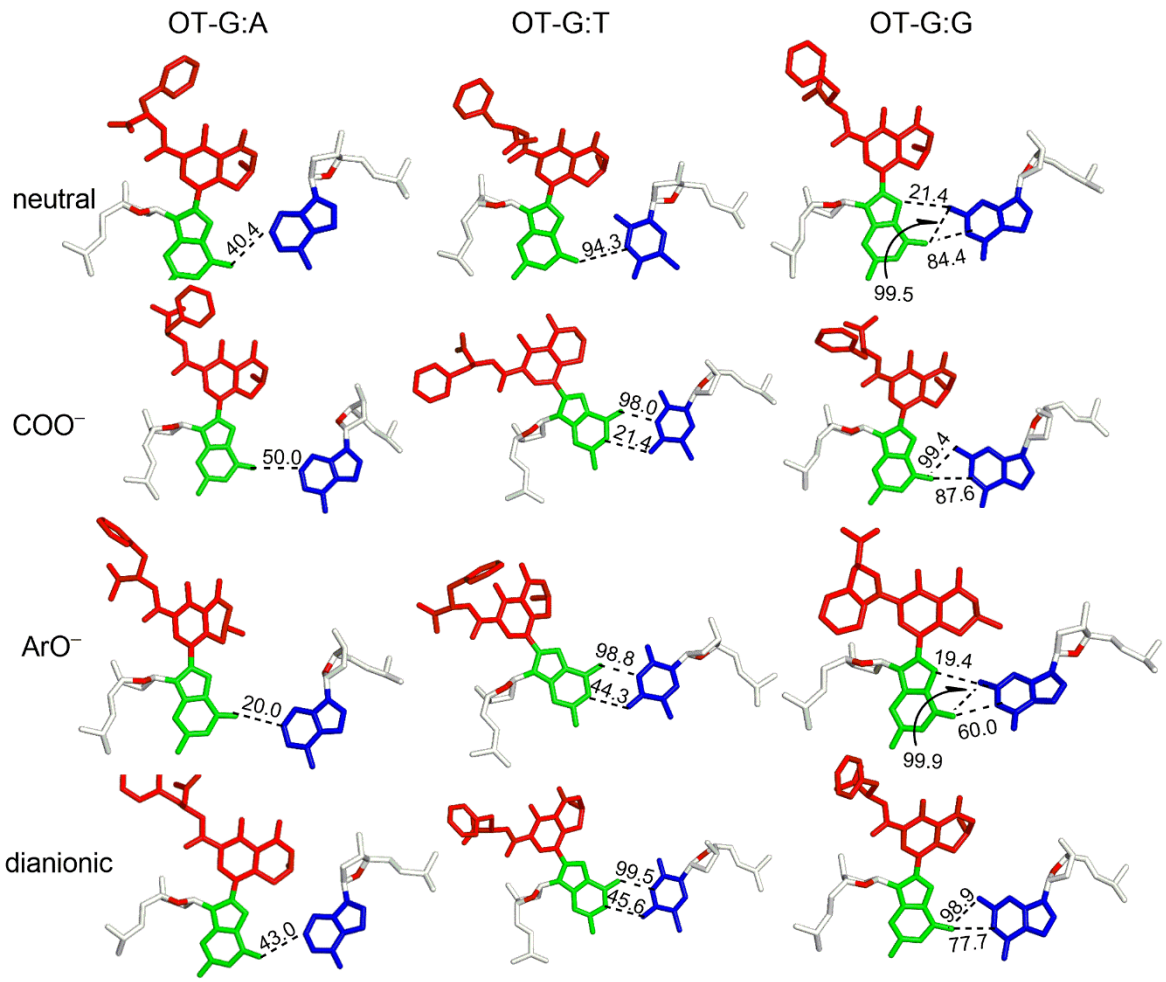

Figure S17. Lesion-site hydrogen bonding for OT-G in different ionization states at the G^1 position mispaired against A, T or G in the W adducted DNA conformation.

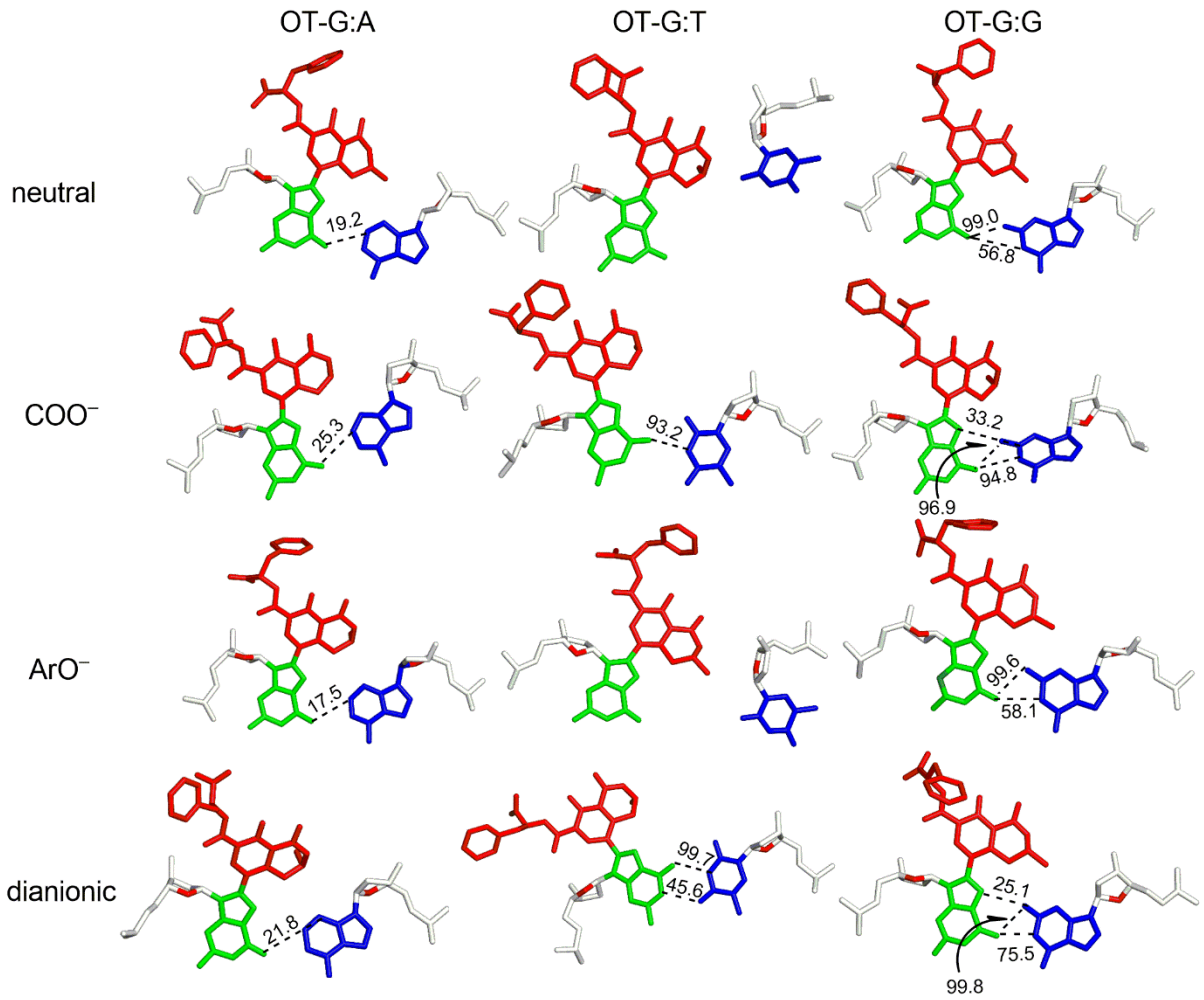

Figure S18. Lesion-site hydrogen bonding for OT-G in different ionization states at the G^2 position mispaired against A, T or G in the W adducted DNA conformation.

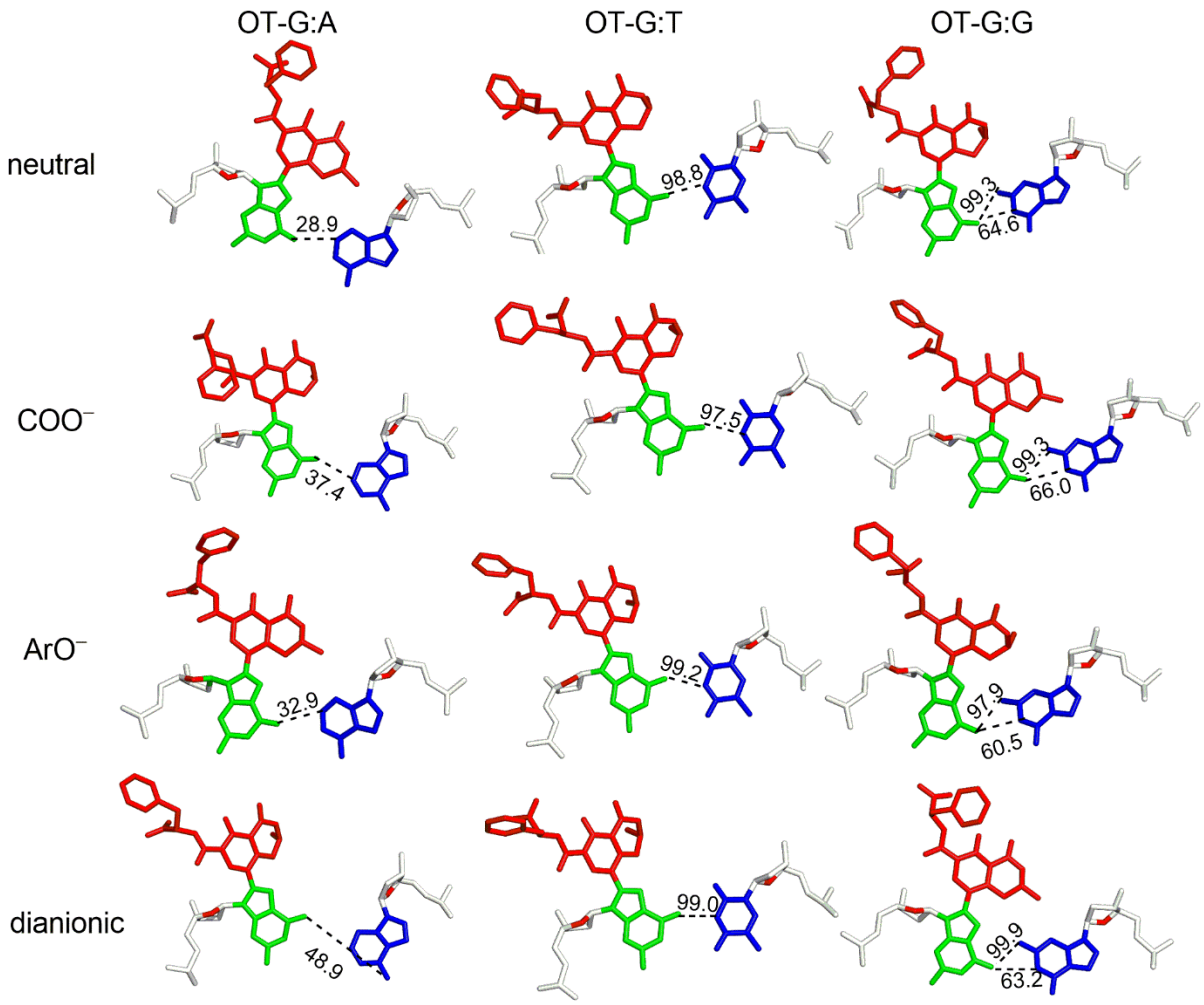

Figure S19. Lesion-site hydrogen bonding for OT-G in different ionization states at the G^3 position mispaired against A, T or G in the W adducted DNA conformation.

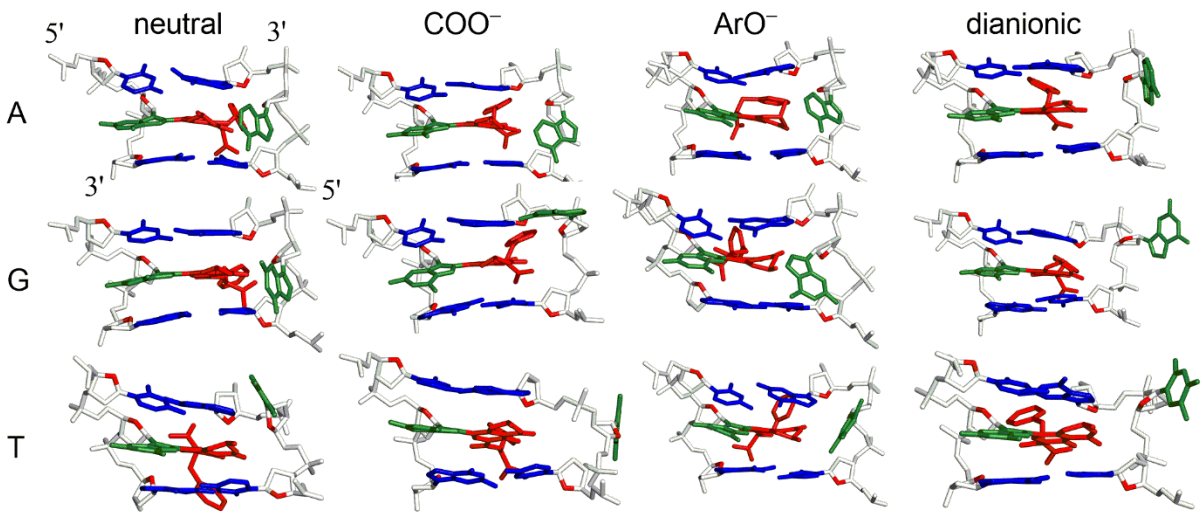

Figure S20. Representative lesion-site structures of the stacked (S) conformers containing OT-G in different ionization states at the G^1 position and paired opposite A, G or T. The OT moiety is shown in red, the damaged G moiety and the opposing base in green, and the base pairs flanking the lesion in blue.

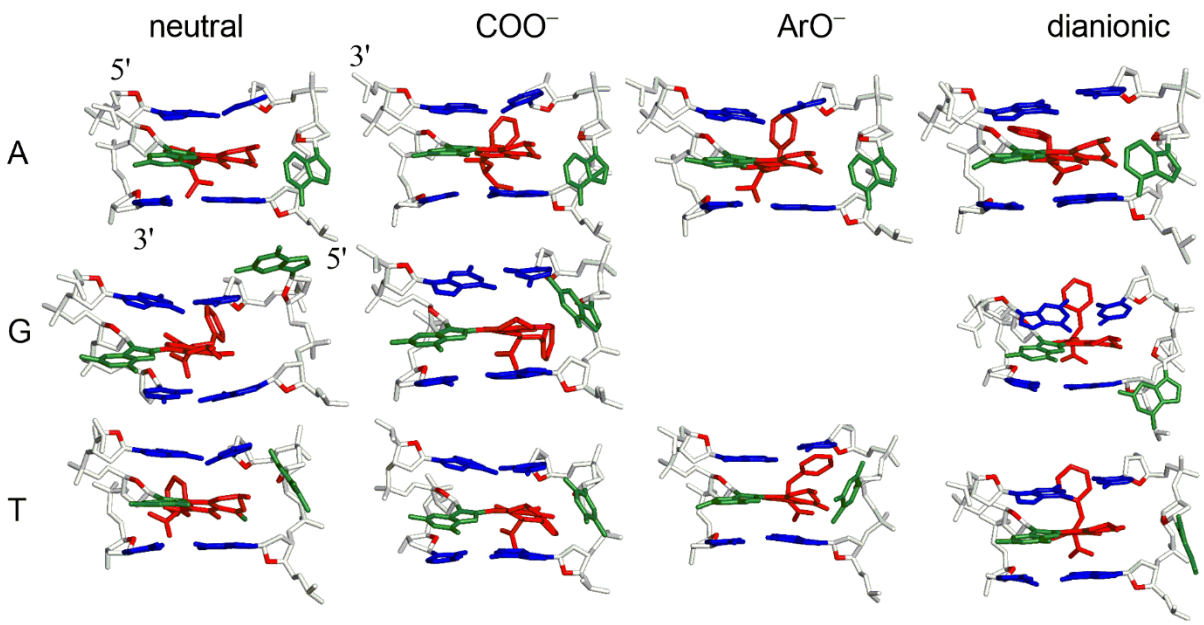

Figure S21. Representative lesion-site structures of the stacked (S) conformers of DNA containing OT-G in different ionization states at the G^2 position and paired opposite A, G or T. The OT moiety is shown in red, the damaged G moiety and the opposing base in green, and the base pairs flanking the lesion in blue.

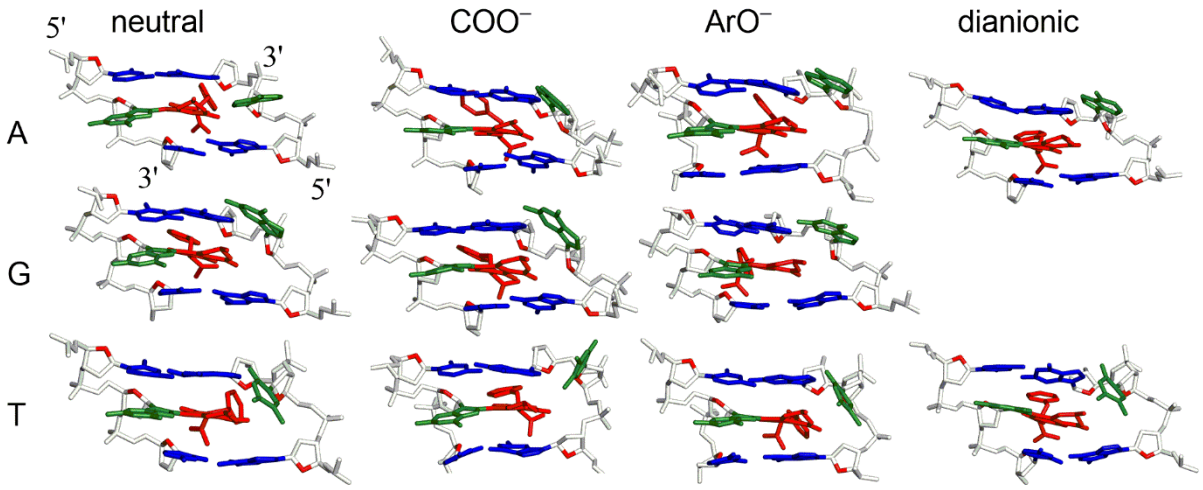

Figure S22. Representative lesion-site structures of the stacked (S) conformers containing OT-G in different ionization states at the G^3 position and paired opposite A, G or T. The OT moiety is shown in red, the damaged G moiety and the opposing base in green, and the base pairs flanking the lesion in blue.

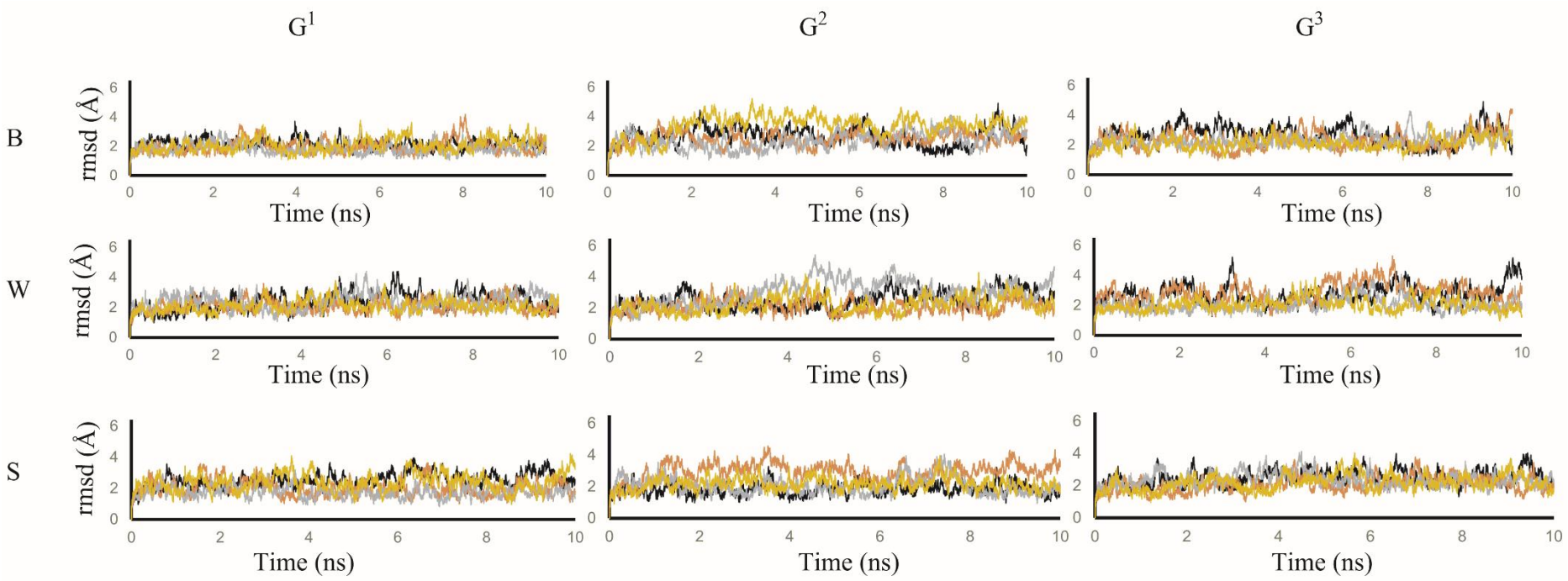

Figure S23. Backbone rmsd (Å) versus time for OT-G in the neutral (grey), COO^- (orange), ArO^- (yellow) and dianionic (black) ionization states mismatched against A in different (B, W and S) DNA conformations and (G^1, G^2 and G^3) sequence contexts.

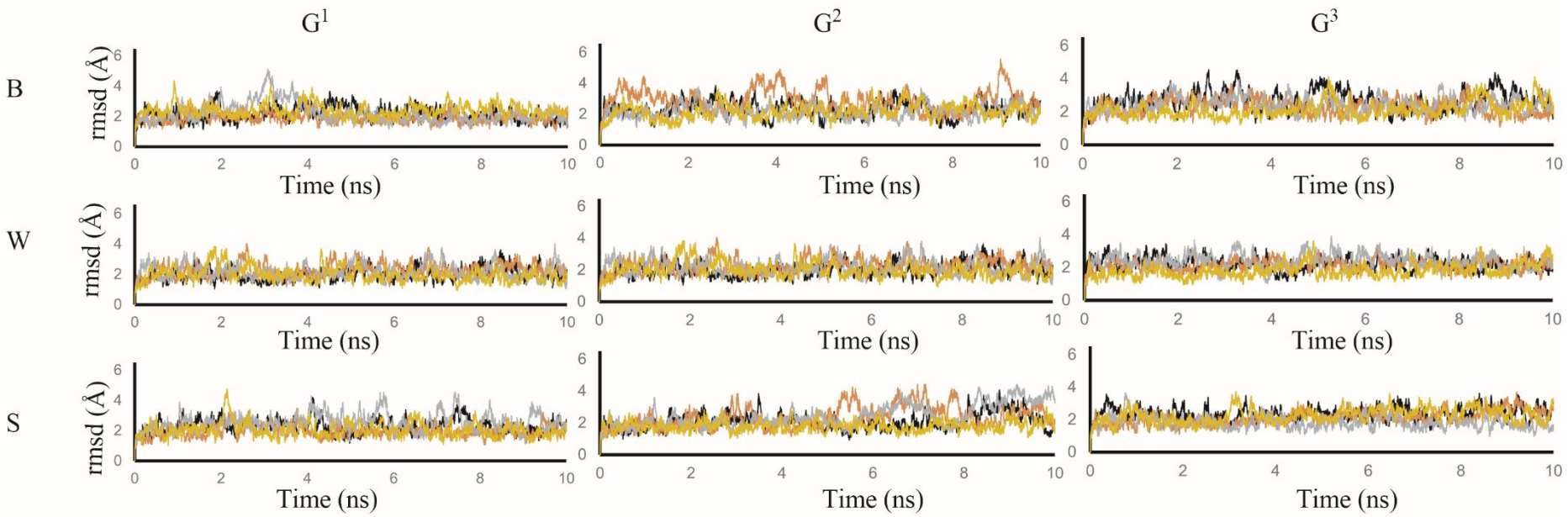

Figure S24. Backbone rmsd (Å) versus time for OT-G in the neutral (grey), COO^- (orange), ArO^- (yellow) and dianionic (black) ionization states mismatched against T in different (B, W and S) DNA conformations and (G^1, G^2 and G^3) sequence contexts.

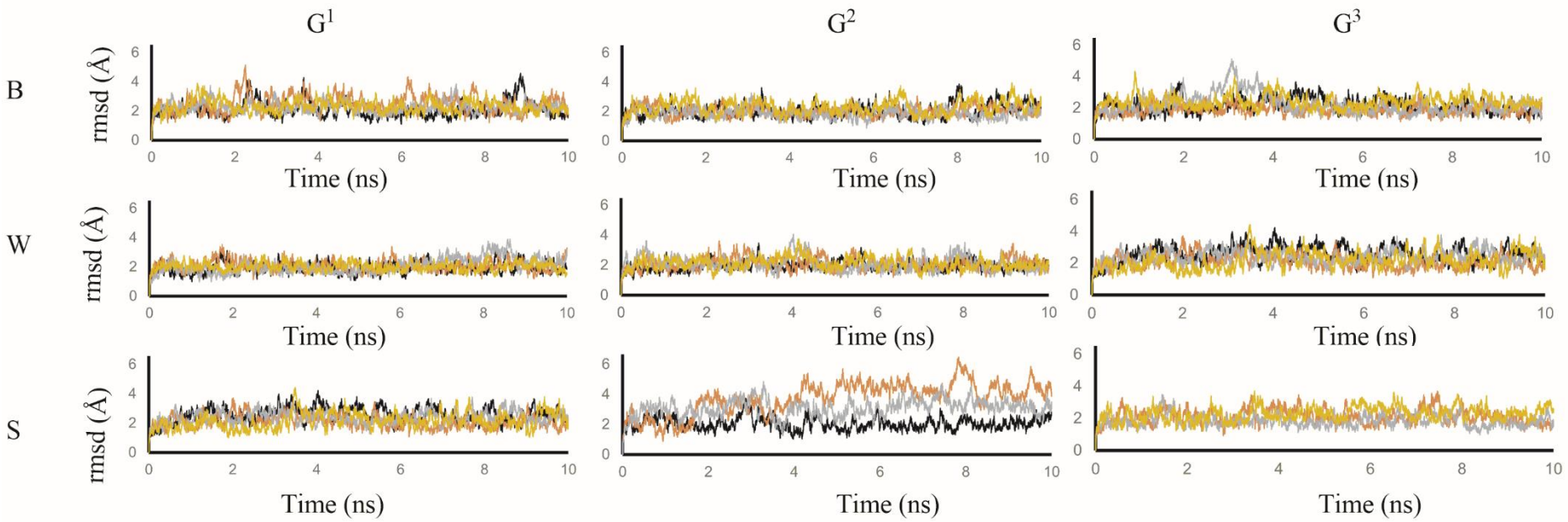

Figure S25. Backbone rmsd (Å) versus time for OT-G in the neutral (grey), COO^- (orange), ArO^- (yellow) and dianionic (black) ionization states mismatched against G in different (B, W and S) DNA conformations and (G^1, G^2 and G^3) sequence contexts.

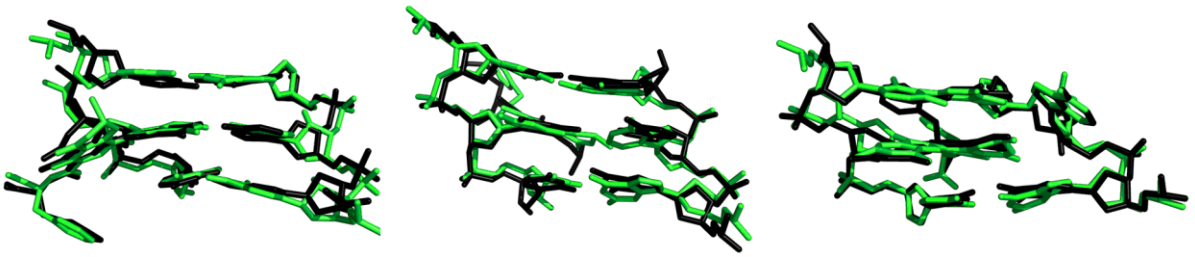

Figure S26. Overlay of the representative structures for the lesion site obtained from the last 10 ns of MD simulations carried out using different non-bonded cut-offs for the B, W and S conformers containing COO^- OT-G at the G^3 position paired opposite A. The representative structures from simulations performed using an 8 Å water box and a non-bonded cut-off of 10 Å are shown in black, whereas those from simulations performed using a 10 Å water box and non-bonded cut-off of 9 Å are shown in green. The rmsd values for the overlaid structures (Å) are provided in parentheses.

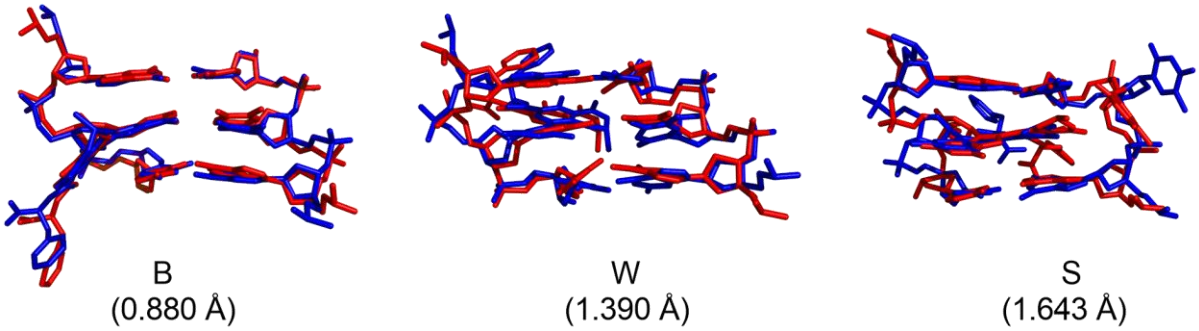

Figure S27. Overlay of the representative structures of the lesion site obtained from 40 ns and 500 ns MD production simulations for the B, W and S conformers containing COO^- OT-G at the G^2 position and paired opposite T. The representative structure from 40 ns are shown in red, whereas those from 500 ns simulations are shown in blue. The rmsd values for the overlaid structures (Å) are provided in parentheses.

Table S1. Average values and standard deviations (in parentheses) for the χ and θ dihedral angles (deg.), and the backbone rmsd (Å) for different conformations of DNA containing different ionization states of OT-G paired against A at G^1, G^2 or G^3.

OT-G Ionization state	Position	Major Groove			Wedge			Stacked		
		χ^a	θ^b	rmsd[c]	χ^a	θ^b	rmsd[c]	χ^a	θ^b	rmsd[c]
Neutral	G^1	207.0 (9.7)	19.3 (6.3)	1.9 (0.4)	74.4 (9.9)	16.3 (6.4)	2.4 (0.5)	42.5 (7.0)	347.5 (5.9)	1.8 (0.4)
COO^-		208.4 (8.0)	18.6 (6.3)	2.0 (0.5)	75.0 (9.6)	17.4 (6.1)	2.1 (0.4)	39.7 (7.1)	347.2 (5.9)	2.0 (0.5)
ArO^-		214.0 (8.9)	15.0 (6.6)	2.1 (0.5)	72.4 (9.8)	20.4 (6.1)	2.1 (0.4)	36.8 (7.4)	349.9 (6.5)	2.4 (0.6)
Dianionic		207.9 (8.3)	19.6 (6.3)	2.1 (0.3)	74.5 (9.2)	14.9 (6.2)	2.4 (0.6)	38.0 (7.2)	347.5 (6.0)	2.5 (0.5)
Neutral	G^2	205.5 (12.5)	17.7 (6.9)	2.3 (0.6)	71.7 (10.8)	18.2 (6.8)	3.0 (0.8)	38.9 (13.0)	352.8 (9.0)	2.6 (0.6)
COO^-		204.4 (10.7)	20.2 (6.3)	2.5 (0.4)	77.5 (9.9)	16.3 (6.7)	2.1 (0.4)	36.0 (7.4)	348.3 (6.0)	3.0 (0.5)
ArO^-		214.5 (11.7)	20.6 (6.3)	3.4 (0.7)	77.3 (9.8)	15.7 (6.8)	2.2 (0.5)	36.8 (7.5)	348.4 (6.1)	2.2 (0.4)
Dianionic		206.0 (9.7)	21.5 (6.3)	2.3 (0.4)	74.8 (9.6)	14.5 (6.5)	2.5 (0.6)	37.4 (7.3)	347.9 (6.1)	1.8 (0.4)
Neutral	G^3	217.5 (7.8)	12.6 (6.3)	2.3 (0.4)	53.4 (21.5)	3.6 (12.1)	2.0 (0.4)	36.0 (8.1)	352.8 (6.5)	2.4 (0.4)
COO^-		209.1 (9.0)	18.2 (6.3)	2.3 (0.6)	77.6 (9.3)	17.0 (6.0)	2.1 (0.5)	34.4 (7.8)	352.0 (6.4)	2.1 (0.5)
ArO^-		211.5 (9.8)	16.9 (6.7)	2.1 (0.4)	68.9 (15.9)	13.1(9.5)	2.1 (0.4)	36.8 (7.2)	348.2 (6.0)	2.2 (0.5)
Dianionic		207.8 (8.8)	19.4 (6.2)	2.2 (0.5)	73.4 (11.1)	18.3 (6.2)	2.6 (0.6)	34.6 (13.6)	356.9 (8.3)	2.5 (0.5)

[a]The dihedral angle χ ($\angle$(O4′C1′N9C4), Figure 1) describes the orientation of the nucleobase with respect to sugar. [b]The dihedral angle θ ($\angle$(N9C8C10C11), Figure 1) describes the orientation of the OT moiety with respect to nucleobase. [c]rmsd is calculated with respect to the first frame of the production run.

Table S2. Average values and standard deviations (in parentheses) for the χ and θ dihedral angles (deg.), and the backbone rmsd (Å) for different conformations of DNA containing different ionization states of OT-G paired against T at G^1, G^2 or G^3.

OT-G Ionization state	Position	Major Groove			Wedge			Stacked		
		χ^a	θ^b	rmsd[c]	χ^a	θ^b	rmsd[c]	χ^a	θ^b	rmsd[c]
Neutral	G^1	219.8 (7.6)	10.2 (6.2)	4.1 (0.8)	74.7 (9.8)	16.7 (6.1)	2.2 (0.5)	38.8 (7.1)	348.2 (6.0)	2.5 (0.6)
COO^-		205.6 (9.2)	18.6 (6.2)	2.1 (0.5)	79.9 (9.6)	16.7 (5.9)	2.3 (0.5)	38.6 (7.1)	346.7 (5.9)	1.9 (0.4)
ArO^-		213.2 (8.7)	13.1 (6.4)	2.3 (0.4)	80.0 (9.6)	17.6 (6.0)	2.2 (0.4)	37.6 (7.3)	348.9 (6.3)	2.0 (0.5)
Dianionic		206.5 (9.9)	19.3 (6.2)	2.2 (0.4)	77.9 (9.4)	17.6 (5.9)	2.0 (0.4)	37.8 (7.2)	347.4 (6.0)	2.3 (0.4)
Neutral	G^2	216.3 (7.6)	11.1 (6.3)	2.1 (0.4)	78.7(8.7)	17.3 (6.0)	3.2 (0.8)	36.7 (7.5)	350.0 (6.5)	2.4 (0.7)
COO^-		203.8 (14.2)	20.2 (6.3)	2.9 (0.7)	77.2 (9.0)	16.0 (5.9)	2.5 (0.9)	36.6 (7.4)	346.9 (6.1)	2.4 (0.7)
ArO^-		211.7 (8.0)	16.1 (6.2)	2.2 (0.5)	78.7 (8.7)	17.3 (6.0)	3.2 (0.8)	35.5 (8.4)	349.4 (6.6)	1.7 (0.3)
Dianionic		214.2 (10.4)	14.2 (7.9)	2.3 (0.5)	74.3 (10.4)	18.0 (6.0)	2.1 (0.4)	37.1 (7.4)	347.8 (6.1)	2.1 (0.5)
Neutral	G^3	220.1 (9.5)	10.0 (7.0)	2.4 (0.4)	78.2 (9.6)	17.0 (6.1)	2.4 (0.5)	36.2 (7.6)	352.4 (6.7)	1.8 (0.4)
COO^-		206.1 (9.5)	18.5 (6.4)	2.3 (0.5)	77.5 (9.8)	17.6 (5.8)	2.1 (0.3)	36.2 (7.3)	349.1 (6.2)	2.1 (0.4)
ArO^-		213.7 (7.9)	14.7 (6.4)	2.1 (0.5)	76.4 (9.9)	18.2 (5.9)	1.8 (0.4)	34.8 (8.0)	352.2 (7.1)	2.3 (0.5)
Dianionic		216.7 (8.7)	10.8 (6.9)	2.7 (0.6)	70.8 (10.4)	18.4 (5.9)	2.2 (0.4)	29.5 (8.6)	358.1 (7.3)	2.2 (0.5)

[a]The dihedral angle χ ($\angle$(O4′C1′N9C4), Figure 1) describes the orientation of the nucleobase with respect to sugar. [b]The dihedral angle θ ($\angle$(N9C8C10C11), Figure 1) describes the orientation of the OT moiety with respect to nucleobase. [c]rmsd is calculated with respect to the first frame of the production run.

Table S3. Average values and standard deviations (in parentheses) for the χ and θ dihedral angles (deg.), and the backbone rmsd (Å) for different conformations of DNA containing different ionization states of OT-G paired against G at G^1, G^2 or G^3.

OT-G Ionization state	Position	Major Groove			Wedge			Stacked		
		χ^a	θ^b	rmsd[c]	χ^a	θ^b	rmsd[c]	χ^a	θ^b	rmsd[c]
Neutral	G^1	210.0 (11.2)	19.0 (7.1)	2.2 (0.4)	77.9 (8.8)	15.8 (6.1)	2.1 (0.5)	43.3 (6.9)	347.1 (5.9)	2.0 (0.4)
COO^-		221.1 (7.8)	11.8 (6.3)	2.5 (0.6)	77.2 (8.8)	16.5 (6.1)	2.1 (0.4)	37.9 (7.2)	347.3 (5.9)	2.3 (0.5)
ArO^-		220.7 (8.2)	12.1 (6.4)	2.3 (0.4)	76.0 (8.8)	16.5 (6.0)	2.0 (0.3)	38.4 (7.6)	348.7 (6.7)	2.6 (0.5)
Dianionic		220.5 (8.5)	14.2 (7.1)	2.1 (0.5)	76.6 (8.7)	15.3 (6.0)	1.9 (0.4)	38.0 (7.2)	347.2 (5.9)	2.3 (0.4)
Neutral	G^2	219.4 (7.2)	13.1 (6.1)	1.9 (0.4)	78.2 (9.1)	14.4 (6.2)	2.1 (0.5)	37.1 (7.7)	350.0 (6.8)	3.1 (0.6)
COO^-		206.5 (10.2)	19.8 (6.5)	2.0 (0.4)	82.9 (8.2)	16.3 (5.9)	1.8 (0.4)	38.1 (7.2)	347.8 (6.0)	3.7 (1.0)
ArO^-		217.9 (8.5)	14.5 (6.5)	2.3 (0.5)	77.9 (9.7)	13.9 (6.4)	2.1 (0.4)	–	–	–
Dianionic		214.5 (7.8)	20.2 (6.7)	2.1 (0.5)	70.0 (19.1)	11.0 (9.4)	2.0 (0.3)	39.1 (7.3)	345.7 (6.2)	2.1 (0.4)
Neutral	G^3	217.9 (7.6)	12.8 (6.2)	2.2 (0.7)	77.9 (8.9)	16.0 (6.1)	2.4 (0.4)	36.5 (7.7)	353.0 (6.3)	1.8 (0.4)
COO^-		219.5 (9.3)	14.0 (7.1)	1.9 (0.3)	77.6 (8.9)	15.7 (6.0)	2.1 (0.4)	32.8 (8.2)	354.0 (6.7)	2.1 (0.5)
ArO^-		217.1 (7.6)	15.0 (6.3)	2.4 (0.4)	74.6 (11.8)	14.9 (7.4)	2.2 (0.6)	35.1 (8.0)	352.4 (7.0)	2.3 (0.4)
Dianionic		214.6 (10.7)	16.2 (7.9)	2.1 (0.5)	75.5 (9.0)	14.8 (5.8)	2.4 (0.5)	–	–	–

[a]The dihedral angle χ ($\angle$(O4′C1′N9C4, Figure 1) describes the orientation of the nucleobase with respect to sugar. [b]The dihedral angle θ ($\angle$(N9C8C10C11), Figure 1) describes the orientation of the OT moiety with respect to nucleobase. [c]rmsd is calculated with respect to the first frame of the production run.

Table S4. Occupancies (%) of the hydrogen bonds in the trimers composed of the OT-G:A mismatch, and the 3′– and 5′–flanking base pairs for the major groove and wedge conformations of damaged DNA.[a]

Position	Base Pair	Hydrogen Bond (D–A)	Major Groove Conformation				Hydrogen Bond (D–A)	Wedge Conformation			
			neutral	COO^-	ArO^-	dianionic		neutral	COO^-	ArO^-	dianionic
G^1	5′C:G	N4(C)–O6(G)	98.7	97.4	99.0	98.1	N4(C)–O6(G)	98.8	99.6	99.5	99.1
		N1(G)–N3(C)	99.9	99.6	99.9	99.9	N1(G)–N3(C)	99.9	100.0	100.0	99.9
		N2(G)–O2(C)	99.8	99.8	99.7	99.8	N2(G)–O2(C)	99.7	99.7	99.9	99.7
	G^1:A	N1(OT-G)–N7(A)	99.8	99.7	99.8	99.6	N6(A)–O6(OT-G)	–	–	–	–
		N6(A)–O6(OT-G)	93.9	94.4	96.1	94.4	C2(A)–O6(OT-G)	40.4	50.0	20.0	43.0
		N2(OT-G)–N7(A)	53.6	50.2	59.4	64.8					
	3′G:C	N4(C)–O6(G)	99.1	98.8	99.2	94.6	N4(C)–O6(G)	98.3	91.9	95.0	98.8
		N1(G)–N3(C)	100.0	100.0	100.0	100.0	N1(G)–N3(C)	99.9	98.7	98.8	100.0
		N2(G)–O2(C)	100.0	99.9	99.9	99.9	N2(G)–O2(C)	99.9	98.7	98.9	99.9
G^2	5′G:C	N4(C)–O6(G)	98.9	98.5	98.5	98.1	N4(C)–O6(G)	99.4	99.1	99.1	99.1
		N1(G)–N3(C)	100.0	99.9	100.0	99.9	N1(G)–N3(C)	100.0	100.0	100.0	99.9
		N2(G)–O2(C)	99.9	99.9	99.8	99.9	N2(G)–O2(C)	99.8	99.8	99.7	99.8
	G^2:A	N1(OT-G)–N7(A)	99.2	99.2	99.0	98.4	N6(A)–O6(OT-G)	–	–	–	–
		N6(A)–O6(OT-G)	97.0	97.9	97.5	98.6	C2(A)–O6(OT-G)	19.2	25.3	17.5	21.8
		N2(OT-G)–N7(A)	41.9	32.4	37.3	36.1	N3 (A)–C14(OT-G)				19.6
	3′C:G	N4(C)–O6(G)	98.5	98.9	97.9	98.8	N4(C)–O6(G)	85.3	87.3	57.9	98.1
		N1(G)–N3(C)	100.0	100.0	99.1	100.0	N1(G)–N3(C)	88.3	90.8	63.1	100.0
		N2(G)–O2(C)	99.8	99.8	99.3	99.8	N2(G)–O2(C)	99.8	99.9	98.8	99.9
G^3	5′C:G	N4(C)–O6(G)	99.5	98.1	98.7	98.2	N4(C)–O6(G)	99.4	97.7	99.1	98.5
		N1(G)–N3(C)	100.0	99.9	99.9	99.9	N1(G)–N3(C)	99.9	98.8	100.0	99.9
		N2(G)–O2(C)	99.8	99.9	99.9	99.9	N2(G)–O2(C)	99.9	99.5	99.9	99.2
	G^3:A	N1(OT-G)–N7(A)	99.5	99.3	99.4	99.3	N6(A)–O6(OT-G)	–	-	–	48.9
		N6(A)–O6(OT-G)	90.4	96.4	96.5	96.7	C2(A)–O6(OT-G)	28.9	37.4	32.9	–
		N2(OT-G)–N7(A)	80.0	37.2	56.0	53.0					
	3′C:G	N4(C)–O6(G)	98.2	98.8	98.4	98.7	N4(C)–O6(G)	98.6	88.6	90.1	95.7

		N1(G)–N3(C)	100.0	100.0	100.0	99.9	N1(G)–N3(C)	100.0	97.1	96.3	95.9
		N2(G)–O2(C)	99.6	99.8	99.7	99.7	N2(G)–O2(C)	99.7	99.4	99.7	94.0

[a]Hydrogen-bonding interactions were determined using a cut-off of 3.4 Å for the donor–acceptor distance and 120° for the donor–hydrogen–acceptor angle.

Table S5. Occupancies (%) of the hydrogen bonds in the trimers composed of the OT-G:G mismatch, and the 3′– and 5′–flanking base pairs for the major groove and wedge conformations of damaged DNA.[a]

Position	Base Pair	Hydrogen Bond (D–A)	Major Groove Conformation				Hydrogen Bond (D–A)	Wedge Conformation			
			neutral	COO^-	ArO^-	dianionic		neutral	COO^-	ArO^-	dianionic
G^1	5′C:G	N4(C)–O6(G)	97.6	99.1	99.2	96.1	N4(C)–O6(G)	99.1	98.3	99.0	98.9
		N1(G)–N3(C)	99.8	100.0	100.0	99.8	N1(G)–N3(C)	100.0	99.9	99.9	99.9
		N2(G)–O2(C)	99.7	99.7	99.7	99.4	N2(G)–O2(C)	99.8	99.9	99.9	99.4
	G^1:G	N1(OT-G)–O6(G)	50.0	77.4	76.9	96.5	N1(G)–O6(OT-G)	84.4	87.6	60.0	77.7
		N2(OT-G)–N7(G)	84.2	92.9	94.8	27.9	N2(G)–O6(OT-G)	99.5	99.4	99.9	98.9
		N1(OT-G)–N7(G)	43.3	–	–	–	N2(G)–N7 (OT-G)	21.4	–	19.4	–
		N2(OT-G)–O6(G)	–	22.7	21.6	75.0	N2 (G)–C13 (OT-G)	–	–	33.1	–
	3′G:C	N4(C)–O6(G)	98.7	98.8	98.5	96.7	N4(C)–O6(G)	98.9	98.9	99.0	98.7
		N1(G)–N3(C)	100.0	100.0	99.9	99.7	N1(G)–N3(C)	99.9	100.0	99.9	99.9
		N2(G)–O2(C)	99.8	99.9	99.9	99.8	N2(G)–O2(C)	99.8	99.8	99.9	99.8
G^2	5′G:C	N4(C)–O6(G)	98.8	97.6	98.5	98.9	N4(C)–O6(G)	99.0	97.7	99.3	99.1
		N1(G)–N3(C)	99.9	99.9	99.9	99.9	N1(G)–N3(C)	100.0	100.0	100.0	100.0
		N2(G)–O2(C)	99.9	99.9	99.9	99.8	N2(G)–O2(C)	99.8	98.8	99.8	99.8
	G^2:G	N1(OT-G)–O6(G)	–	–	–	–	N1(G)–O6(OT-G)	56.8	94.8	58.1	75.5
		N2(OT-G)–N7(G)	96.1	84.3	95.1	76.2	N2(G)–O6(OT-G)	99.0	96.9	99.6	99.8
		N1(OT-G)–N7(G)	61.6	71.9	70.1	81.3	N2 (G)–N7 (OT-G)	–	33.2	–	25.1
		N1(OT-G)–O6(G)	–	–	–	–	N2 (G)–C13 (OT-G)	–	–	24.0	30.2
	3′C:G	N4(C)–O6(G)	98.4	98.0	98.1	97.3	N4(C)–O6(G)	95.1	93.2	98.4	98.4
		N1(G)–N3(C)	100.0	100.0	100.0	100.0	N1(G)–N3(C)	99.5	99.6	99.9	99.8
		N2(G)–O2(C)	99.8	99.8	99.8	99.9	N2(G)–O2(C)	98.4	99.5	99.4	99.6
	5′C:G	N4(C)–O6(G)	99.4	97.4	99.2	97.9	N4(C)–O6(G)	99.3	99.2	98.6	99.3
		N1(G)–N3(C)	100.0	99.7	99.9	99.9	N1(G)–N3(C)	100.0	100.0	99.9	99.9
		N2(G)–O2(C)	99.8	99.8	99.8	99.8	N2(G)–O2(C)	99.8	99.8	99.9	99.9
	G^3:G	N1(OT-G)–O6(G)	64.8	91.2	–	52.1	N1(G)–O6(OT-G)	64.6	66.0	60.5	63.2
		N2(OT-G)–N7(G)	98.4	48.3	97.0	61.0	N2(G)–O6(OT-G)	99.3	99.3	97.9	99.9

G^3		N1(OT-G)–N7(G)	38.2	–	67.8	42.8					
		N2(OT-G)–O6(G)	–	47.5	–	–				–	–
	3′C:G	N4(C)–O6(G)	97.0	97.1	96.8	96.7	N4(C)–O6(G)	95.3	95.9	92.7	97.9
		N1(G)–N3(C)	99.9	99.5	100.0	99.9	N1(G)–N3(C)	99.4	99.6	97.6	99.8
		N2(G)–O2(C)	99.7	99.9	99.7	99.7	N2(G)–O2(C)	99.4	99.5	99.5	99.5

[a]Hydrogen-bonding interactions were determined using a cut-off of 3.4 Å for the donor–acceptor distance and 120° for the donor–hydrogen–acceptor angle.

Table S6: Occupancies (%) of the hydrogen bonds in the trimers composed of the OT-G:T mismatch, and the 3′– and 5′–flanking base pairs for the major groove and wedge conformations of damaged DNA.[a]

Position	Base Pair	Hydrogen Bond (D–A)	Major Groove Conformation				Hydrogen Bond (D–A)	Wedge Conformation			
			neutral	COO^-	ArO^-	dianionic		neutral	COO^-	ArO^-	dianionic
G^1	5′C:G	N4(C)–O6(G)	99.0	98.3	98.8	97.8	N4(C)–O6(G)	95.6	99.2	98.3	98.9
		N1(G)–N3(C)	100.0	99.9	100.0	100.0	N1(G)–N3(C)	100.0	100.0	99.9	100.0
		N2(G)–O2(C)	99.9	99.8	100.0	99.9	N2(G)–O2(C)	99.8	99.5	99.3	99.6
	G^1:T	N2(OT-G)–O2(T)	94.8	32.0	36.2	42.4	N3(T)–O6(OT-G)	94.3	98.0	98.8	99.5
		N1(OT-G)–O2(T)	97.4	99.7	99.9	99.7	O4(T)–N1(OT-G)	–	21.4	44.3	45.6
		O6(OT-G)–N3(T)	–	86.4	92.8	86.7					
	3′G:C	N4(C)–O6(G)	97.8	96.8	98.8	95.4	N4(C)–O6(G)	98.5	99.0	98.9	99.3
		N1(G)–N3(C)	99.9	100.0	100.0	100.0	N1(G)–N3(C)	99.9	100.0	99.9	100.0
		N2(G)–O2(C)	99.7	99.8	99.8	99.8	N2(G)–O2(C)	99.8	99.7	99.7	99.6
G^2	5′G:C	N4(C)–O6(G)	99.1	99.1	99.4	99.1	N4(C)–O6(G)	99.4	95.6	98.6	98.1
		N1(G)–N3(C)	99.9	99.9	100.0	100.0	N1(G)–N3(C)	100.0	99.9	100.0	99.9
		N2(G)–O2(C)	99.9	99.8	100.0	99.9	N2(G)–O2(C)	99.8	99.2	99.8	99.8
	G^2:T	N2(OT-G)–O2(T)	29.2	–	30.1	–	N3(T)–O6(OT-G)	–	93.2	–	99.7
		N1(OT-G)–O2(T)	99.8	87.4	100.0	88.1	O4 (T)–N1(OT-G)	–	–	–	45.6
		O6(OT-G)–N3(T)	96.4	99.7	98.7	99.4					
	3′C:G	N4(C)–O6(G)	98.3	98.5	98.9	98.5	N4(C)–O6(G)	22.4	97.4	98.2	99.0
		N1(G)–N3(C)	100.0	99.7	100.0	100.0	N1(G)–N3(C)	50.4	99.8	99.9	99.9
		N2(G)–O2(C)	99.9	100.0	99.8	99.6	N2(G)–O2(C)	25.3	97.4	99.9	99.3
G^3	5′C:G	N4(C)–O6(G)	98.0	97.7	99.0	97.7	N4(C)–O6(G)	95.4	99.2	99.1	99.1
		N1(G)–N3(C)	99.8	100.0	100.0	99.8	N1(G)–N3(C)	99.9	99.9	99.9	100.0
		N2(G)–O2(C)	99.9	99.9	100.0	100.0	N2(G)–O2(C)	99.3	99.7	99.5	99.8
	G^3:T	N2(OT-G)–O2(T)	26.9	–	39.2	22.0	N3(T)–O6(OT-G)	98.8	97.5	99.2	99.0
		N1(OT-G)–O2(T)	99.1	97.1	99.8	99.6					
		O6(OT-G)–N3(T)	86.1	98.3	92.3	97.8					
	3′C:G	N4(C)–O6(G)	98.1	98.4	98.3	98.3	N4(C)–O6(G)	97.6	99.2	99.3	98.9

		N1(G)–N3(C)	99.9	99.9	99.8	99.9	N1(G)–N3(C)	99.7	99.9	99.9	99.7
		N2(G)–O2(C)	99.8	99.8	99.7	99.6	N2(G)–O2(C)	99.6	99.0	99.5	98.8

[a]Hydrogen-bonding interactions were determined using a cut-off of 3.4 Å for the donor–acceptor distance and 120° for the donor–hydrogen–acceptor angle.

Table S7. Hydrogen-bonding energies (kcal mol^{-1}) between the OT-G and opposing base for different conformations of adducted DNA containing OT-G paired against C, A, T and G.

Position (conformer)	Ionization State	Hydrogen Bonding Energies			
		C[a]	A	T	G
G^1 (Major Groove)	Neutral	−27.1	−12.5 (2.3)	−12.7 (1.8)	−10.8 (4.7)
	COO^-	−25.4	−12.3 (2.3)	−12.9 (2.1)	−11.8 (3.8)
	ArO^-	−25.2	−13.2 (2.3)	−13.8 (2.1)	−10.8 (3.9)
	Dianionic	−23.2	−13.1(2.5)	−11.7 (2.2)	−11.6 (2.6)
G^2 (Major Groove)	Neutral	−27.2	−12.7 (2.2)	−14.6 (2.0)	−8.9 (3.6)
	COO^-	−25.0	−12.5 (2.2)	−11.2 (2.5)	−4.9 (3.7)
	ArO^-	−24.9	−12.8 (2.3)	−13.6 (2.0)	−5.2 (3.1)
	Dianionic	−22.6	−13.6 (2.4)	−9.6 (2.5)	−0.5 (3.2)
G^3 (Major Groove)	Neutral	−27.2	−12.7 (2.3)	−14.2 (2.1)	−11.1 (3.9)
	COO^-	−25.1	−12.2 (2.3)	−12.1 (2.2)	−12.9 (3.8)
	ArO^-	−25.4	−13.0 (2.3)	−13.1 (2.1)	−5.7 (3.3)
	Dianionic	−22.8	−13.0 (2.4)	−12.1 (2.1)	−6.4 (5.8)
G^1 (Wedge)	Neutral	−9.7	−0.2 (0.8)	−6.0 (1.7)	−11.8 (1.5)
	COO^-	−9.7	1.2 (0.3)	−6.6 (3.3)	−13.8 (1.7)
	ArO^-	−5.9	2.3 (0.9)	−7.7 (3.9)	−13.9 (1.7)
	Dianionic	−7.0	4.3 (0.8)	−7.1 (3.7)	−18.3 (2.1)
G^2 (Wedge)	Neutral	−10.0	1.1 (0.8)	0.0 (1.0)	−11.4 (1.8)
	COO^-	0.9	1.1 (0.8)	−2.5 (3.4)	−13.6 (1.7)
	ArO^-	−0.2	3.1 (0.8)	0.8 (1.0)	−14.1 (2.0)
	Dianionic	3.9	−7.9 (1.2)	−7.2 (3.7)	−17.7 (2.1)
G^3 (Wedge)	Neutral	−2.0	−0.4 (0.9)	−6.8 (2.2)	−11.5 (1.6)
	COO^-	−10.9	2.1 (0.7)	−5.4 (3.1)	−13.3 (1.7)
	ArO^-	−8.1	3.1 (0.8)	−6.3 (3.1)	−14.1 (2.0)
	Dianionic	−9.0	2.5 (4.4)	−4.5 (3.2)	−14.0 (1.8)

[a]Data for C match has been taken from reference 19 of the manuscript.

Table S8. van der Waals stacking energies (kcal mol^{-1}) for different conformations of adducted DNA containing OT-G paired against C, A, T and G.

Position (conformer)	Ionization State	Stacking Energies			
		C[a]	A	T	G
G^1 (Major Groove)	Neutral	–33.4	–33.5 (1.5)	–31.6 (2.0)	–32.9 (1.9)
	COO^-	–33.1	–33.3 (1.6)	–33.9 (1.6)	–33.2 (1.9)
	ArO^-	–33.0	–33.7 (1.6)	–33.4 (1.9)	–33.3 (1.8)
	Dianionic	–33.2	–33.1 (1.8)	–33.9 (1.6)	–31.2 (1.9)
G^2 (Major Groove)	Neutral	–33.4	–36.6 (2.0)	–35.1 (2.1)	–34.7 (1.7)
	COO^-	–34.8	–35.2 (1.8)	–33.9 (1.9)	–34.6 (1.6)
	ArO^-	–33.7	–35.6 (1.7)	–34.4 (1.6)	–34.7 (1.6)
	Dianionic	–32.7	–30.2 (1.6)	–33.7 (1.6)	–33.5 (1.7)
G^3 (Major Groove)	Neutral	–34.1	–34.4 (1.9)	–34.9 (2.4)	–34.2 (1.8)
	COO^-	–33.1	–34.4 (1.7)	–33.7 (1.7)	–31.9 (1.9)
	ArO^-	–34.4	–34.4 (1.6)	–32.9 (2.0)	–34.2 (1.7)
	Dianionic	–33.0	–33.0 (1.5)	–34.1 (1.9)	–31.7 (2.3)
G^1 (Wedge)	Neutral	–37.4	–36.2 (1.8)	–36.1 (1.5)	–38.3 (1.6)
	COO^-	–38.3	–32.2 (1.8)	–32.5 (2.5)	–38.7 (1.6)
	ArO^-	–31.4	–31.8 (2.0)	–31.9 (1.6)	–38.5 (1.6)
	Dianionic	–34.8	–35.4 (1.5)	–30.9(1.9)	–37.7 (1.9)
G^2 (Wedge)	Neutral	–36.7	–21.0 (1.5)	–36.5 (1.9)	–38.5 (1.7)
	COO^-	–29.3	–38.6 (1.9)	–32.6 (1.8)	–39.3 (1.6)
	ArO^-	–34.5	–38.5 (1.8)	–33.8 (2.0)	–38.5 (1.7)
	Dianionic	–29.0	–32.7 (1.7)	–30.5 (1.8)	–38.6 (1.7)
G^3 (Wedge)	Neutral	–32.2	–36.6 (1.8)	–33.8 (2.5)	–38.1 (1.7)
	COO^-	–38.4	–31.7 (1.9)	–30.6 (1.7)	–38.1 (1.6)
	ArO^-	–31.1	–36.4 (1.7)	–31.1 (1.8)	–37.6 (1.8)
	Dianionic	–31.4	–29.2 (2.3)	–30.1 (1.6)	–36.9 (1.5)
G^1 (Stacked)	Neutral	–38.0	–33.8 (1.4)	–35.8 (1.5)	–38.5 (1.4)
	COO^-	–37.2	–35.3 (1.4)	–37.1 (1.5)	–36.6 (1.5)
	ArO^-	–34.2	–31.3 (2.1)	–33.0 (1.7)	–31.8 (1.9)
	Dianionic	–36.2	–35.1(1.5)	–36.3 (1.4)	–36.6 (1.4)
G^2 (Stacked)	Neutral	–33.1	–33.6 (1.7)	–35.1 (1.8)	–34.2 (1.8)
	COO^-	–33.6	–34.0 (1.7)	–35.0 (1.9)	–35.1 (2.0)
	ArO^-	–32.9	–33.4 (1.7)	–33.5 (1.6)	–
	Dianionic	–32.3	–32.0 (1.6)	–32.6 (1.9)	–30.9 (1.9)
G^3 (Stacked)	Neutral	–35.7	–34.9 (1.6)	–34.2 (1.7)	–35.4 (1.5)
	COO^-	–35.4	–34.5 (1.9)	–35.7 (1.5)	–35.1 (1.6)
	ArO^-	–34.3	–36.3 (1.5)	–34.1(1.7)	–34.8 (1.6)
	Dianionic	–33.4	–33.2 (1.8)	–31.9 (1.9)	–

[a]Data for C match has been taken from reference 19 of the manuscript.

Table S9. Average values and standard deviations (in parentheses) for lesion-site pseudostep parameters[a] and minor groove dimension for DNA containing the OT-G adduct paired against A.

Position (Conformer)	Ionization State	Shift (Å)	Slide (Å)	Rise (Å)	Tilt (°)	Roll (°)	Twist (°)	Minor Groove (Å)
G^1 (Major Groove)	Neutral	–0.3 (0.7)	–1.4 (0.8)	6.2 (0.4)	3.0 (4.8)	8.6 (6.6)	54.3 (5.4)	7.9 (1.1)
	COO^-	0.1 (0.8)	–1.9 (0.8)	6.3 (0.4)	3.9 (4.9)	9.2 (7.2)	51.2 (6.2)	8.2 (1.2)
	ArO^-	–0.2 (0.8)	–2.0 (1.0)	6.6 (0.4)	2.1 (5.0)	5.7 (7.3)	58.4 (5.7)	7.2 (1.4)
	Dianionic	0.2 (0.8)	–1.7 (0.9)	6.4 (0.4)	3.9 (4.8)	8.6 (7.0)	51.4 (6.0)	8.1 (1.2)
G^2 (Major Groove)	Neutral	0.3 (0.7)	–1.7 (0.9)	6.7 (0.4)	1.6 (4.9)	3.3 (7.1)	62.4 (6.9)	6.3 (1.7)
	COO^-	0.7 (0.7)	–2.3 (0.7)	6.7 (0.3)	3.1 (4.7)	5.3 (7.1)	57.3 (5.4)	6.9 (1.5)
	ArO^-	0.5 (0.8)	–2.0 (0.8)	6.6 (0.3)	2.3 (4.9)	5.6 (7.4)	57.2 (5.8)	7.2 (1.4)
	Dianionic	1.2 (0.7)	–2.3 (0.7)	6.7 (0.4)	3.0 (4.8)	10.0 (7.6)	52.0 (6.3)	7.6 (1.8)
G^3 (Major Groove)	Neutral	–0.1 (0.9)	–2.6 (0.7)	6.8 (0.4)	5.2 (4.8)	3.3 (7.9)	62.4 (4.3)	5.9 (1.6)
	COO^-	0.0 (0.7)	–1.4 (1.0)	6.3 (0.4)	6.2 (4.9)	3.7 (7.0)	54.4 (6.9)	7.7 (1.4)
	ArO^-	–0.2 (0.9)	–2.1 (1.0)	6.7 (0.5)	4.2 (4.9)	2.1 (7.9)	57.9 (6.1)	6.5 (1.7)
	Dianionic	0.1 (0.7)	–1.6 (0.8)	6.4 (0.4)	5.4 (4.9)	4.5 (6.5)	54.6 (6.8)	7.6 (1.5)
G^1 (Wedge)	Neutral	0.6 (0.8)	–2.7 (0.6)	6.6 (0.4)	1.6 (5.1)	22.6 (9.2)	50.4 (5.6)	9.3 (1.4)
	COO^-	1.6 (0.7)	–1.4 (0.5)	6.1 (0.5)	11.9 (6.3)	13.3 (7.0)	67.2 (4.8)	7.7 (0.9)
	ArO^-	1.6 (0.8)	–1.4 (0.5)	6.5 (0.5)	13.4 (7.0)	14.2 (8.1)	70.1 (6.6)	7.4 (1.1)
	Dianionic	0.4 (0.7)	–2.9 (0.6)	6.6 (0.4)	0.1 (4.9)	20.3 (7.8)	49.3 (5.4)	9.3 (1.1)
G^2 (Wedge)	Neutral	1.0 (1.1)	–2.1 (1.0)	7.0 (0.5)	0.2 (5.1)	29.9 (16.4)	59.2 (7.0)	10.7 (2.3)
	COO^-	0.8 (1.1)	–1.7 (0.9)	6.9 (0.4)	0.1 (5.2)	20.4 (8.4)	60.3 (5.3)	9.7 (1.5)
	ArO^-	1.5 (1.3)	–1.9 (1.0)	6.8 (0.4)	1.3 (5.6)	16.4 (7.7)	61.7 (6.6)	9.3 (1.4)
	Dianionic	0.3 (0.9)	–2.0 (0.7)	7.0 (0.4)	–0.4 (5.0)	19.0 (7.6)	60.5 (4.7)	9.6 (1.6)
G^3 (Wedge)	Neutral	0.3 (0.9)	–2.8 (0.9)	6.8 (0.5)	1.7 (6.0)	14.8 (6.6)	59.9 (6.4)	7.9 (1.0)
	COO^-	0.5 (0.8)	–1.8 (0.8)	6.3 (0.4)	1.3 (5.1)	15.2 (6.1)	59.1 (6.6)	7.9 (1.3)
	ArO^-	0.0 (1.0)	–2.7 (0.6)	6.7 (0.4)	0.8 (5.0)	19.9 (8.7)	55.0 (4.7)	9.6 (1.2)
	Dianionic	–0.7 (0.9)	–1.3 (1.0)	6.4 (0.5)	1.0 (5.5)	20.0 (10.9)	52.8 (6.1)	9.6 (1.5)
G^1 (Stacked)	Neutral	0.8 (0.6)	–0.4 (0.6)	7.0 (0.3)	–1.3 (4.3)	13.4 (5.4)	21.8 (7.2)	11.8 (1.3)
	COO^-	0.8 (0.6)	–0.6 (0.6)	7.0 (0.3)	–0.3 (4.4)	14.2 (5.3)	25.6 (6.6)	11.4 (1.1)
	ArO^-	0.0 (0.7)	–0.5 (0.9)	7.3 (0.4)	–3.1 (5.0)	14.4 (6.5)	29.6 (6.1)	12.2 (0.8)

	Dianionic	1.4 (0.7)	–0.5 (0.7)	7.3 (0.3)	6.5 (5.6)	15.5 (5.9)	46.9 (7.0)	10.6 (1.0)
G^2 (Stacked)	Neutral	–0.5 (0.6)	1.2 (0.7)	6.6 (0.4)	–2.8 (5.2)	9.6 (5.0)	43.2 (4.5)	10.6 (1.3)
	COO^-	–0.6 (0.7)	1.1 (0.6)	6.8 (0.4)	–2.7 (4.9)	10.0 (6.5)	36.5 (5.9)	12.4 (1.1)
	ArO^-	–0.5 (0.6)	1.1 (0.7)	6.6 (0.4)	–2.0 (5.3)	11.3 (6.8)	41.3 (5.2)	11.8 (1.1)
	Dianionic	–0.7 (0.7)	1.1 (0.6)	6.7 (0.4)	–3.4 (5.0)	12.2 (5.8)	35.6 (5.7)	12.3 (1.1)
G^3 (Stacked)	Neutral	1.2 (0.6)	–3.1 (0.9)	7.1 (0.3)	4.4 (5.3)	13.1 (6.2)	60.4 (7.0)	7.4 (0.8)
	COO^-	1.0 (0.7)	–3.6 (1.0)	7.1 (0.4)	1.5 (6.7)	13.5 (6.0)	57.4 (8.3)	7.7 (0.9)
	ArO^-	1.1 (0.5)	0.3 (0.8)	7.3 (0.4)	8.0 (5.2)	11.9 (5.0)	54.7 (5.5)	9.5 (1.2)
	Dianionic	1.2 (0.7)	–3.3 (0.9)	7.3 (0.4)	2.9 (5.0)	10.8 (7.4)	60.5 (6.7)	8.0 (0.9)

[a]Pseudostep parameters at the lesion site were calculated using a base-step consisting of the 5′– and 3′–base pairs with respect to the OT-G adduct.

Table S10. Average values and standard deviations (in parentheses) for lesion-site pseudostep parameters[a] and minor groove dimension for DNA containing the OT-G adduct paired against T.

Position (Conformer)	Ionization State	Shift (Å)	Slide (Å)	Rise (Å)	Tilt (°)	Roll (°)	Twist (°)	Minor Groove (Å)
G^1 (Major Groove)	Neutral	0.2 (0.7)	–2.1 (0.7)	6.7 (0.4)	3.8 (5.3)	21.1 (7.8)	57.9 (6.2)	8.3 (1.1)
	COO^-	–0.1 (0.7)	–1.8 (0.6)	6.1 (0.4)	3.6 (4.9)	8.9 (7.6)	51.7 (6.0)	8.0 (1.4)
	ArO^-	–1.0 (0.8)	–3.4 (0.8)	7.1 (0.6)	0.9 (5.7)	2.7 (7.9)	61.1 (6.4)	6.1 (1.4)
	Dianionic	–0.1 (0.7)	–1.7 (0.7)	6.1 (0.4)	2.9 (5.1)	10.5 (7.3)	48.5 (6.8)	8.7 (1.3)
G^2 (Major Groove)	Neutral	0.0 (0.7)	–2.8 (0.7)	6.7 (0.3)	1.3 (4.8)	4.9 (6.2)	61.9 (4.7)	7.1 (1.5)
	COO^-	0.9 (0.8)	–2.1 (0.7)	6.5 (0.3)	1.6 (4.9)	2.4 (7.3)	58.0 (5.5)	7.4 (1.6)
	ArO^-	–0.7 (0.6)	–3.4 (0.7)	6.7 (0.3)	2.4 (4.6)	1.8 (6.1)	61.4 (4.4)	7.0 (1.3)
	Dianionic	1.2 (0.7)	–2.2 (0.6)	6.5 (0.3)	1.4 (4.8)	5.5 (7.0)	54.2 (4.6)	7.6 (1.4)
G^3 (Major Groove)	Neutral	–0.7 (1.0)	–3.0 (0.9)	6.7 (0.5)	1.0 (5.2)	6.0 (7.3)	55.8 (6.5)	7.2 (1.6)
	COO^-	0.1 (0.8)	–1.4 (0.8)	6.1 (0.4)	5.7 (5.0)	1.9 (6.7)	56.8 (8.3)	7.9 (1.5)
	ArO^-	–0.8 (0.8)	–3.2 (0.8)	7.1 (0.5)	–0.3 (5.0)	–0.5 (7.8)	59.2 (5.2)	6.3 (1.4)
	Dianionic	–1.3 (0.7)	–3.0 (0.8)	7.0 (0.5)	–0.7 (4.9)	5.2 (7.4)	60.5 (5.5)	6.7 (1.5)
G^1 (Wedge)	Neutral	0.9 (0.8)	–1.8 (0.7)	6.5 (0.4)	2.1 (5.0)	14.8 (7.4)	61.1 (5.0)	7.8 (1.0)
	COO^-	0.6 (0.8)	–1.0 (0.9)	6.4 (0.4)	–0.5 (5.3)	12.2 (6.6)	58.1 (5.7)	8.4 (1.1)
	ArO^-	0.6 (0.8)	–0.1 (0.8)	6.3 (0.4)	–1.2 (5.0)	8.8 (6.9)	57.7 (4.9)	9.2 (0.9)
	Dianionic	0.3 (0.8)	–0.5 (0.9)	6.4 (0.4)	–1.4 (5.1)	12.2 (6.8)	56.8 (5.4)	9.2 (1.0)
G^2 (Wedge)	Neutral	Base	pair	broken				8.5 (1.2)
	COO^-	–0.2 (0.6)	0.7 (0.9)	5.8 (0.4)	–0.6 (6.0)	–1.5 (7.3)	70.3 (6.4)	6.6 (1.7)
	ArO^-	–0.2 (0.8)	–2.2 (0.8)	7.0 (0.4)	–2.5 (5.1)	9.6 (6.5)	57.2 (5.9)	9.1 (1.2)
	Dianionic	0.0 (1.0)	0.3 (1.1)	6.3 (0.4)	2.5 (6.6)	8.1 (7.4)	64.4 (6.3)	9.8 (1.2)
G^3 (Wedge)	Neutral	0.9 (0.9)	–1.0 (1.1)	6.3 (0.4)	4.0 (4.7)	10.7 (6.5)	62.6 (4.5)	7.9 (1.2)
	COO^-	0.0 (0.8)	–0.4 (0.8)	6.1 (0.3)	2.7 (5.0)	10.1 (6.7)	58.2 (5.9)	9.0 (0.9)
	ArO^-	0.2 (1.0)	–0.1 (0.9)	6.2 (0.4)	2.2 (4.8)	9.6 (6.8)	60.1 (5.2)	9.0 (0.9)
	Dianionic	–0.4 (0.8)	–0.5 (0.8)	6.2 (0.3)	2.3 (5.0)	12.2 (6.8)	58.2 (5.3)	9.4 (0.9)
G^1 (stacked)	Neutral	1.7 (0.9)	–1.3 (0.7)	7.4 (0.4)	11.9 (5.6)	18.0 (6.2)	61.0 (5.5)	9.0 (1.1)
	COO^-	0.8 (0.6)	–1.1 (0.6)	7.2 (0.3)	4.2 (5.0)	16.7 (5.4)	39.0 (5.5)	10.3 (1.0)
	ArO^-	0.4 (0.8)	–1.5 (0.7)	7.3 (0.4)	2.3 (5.2)	11.5 (6.1)	41.1 (7.1)	10.8 (1.0)

	Dianionic	1.4 (0.6)	0.2 (0.7)	7.3 (0.3)	6.3 (5.2)	10.5 (5.8)	46.3 (5.1)	10.2 (0.9)
G^2 (stacked)	Neutral	–0.1 (0.7)	0.7 (1.5)	6.8 (0.4)	–2.5 (5.8)	5.4 (6.2)	50.0 (7.4)	9.5 (1.5)
	COO^-	–0.2 (0.7)	0.9 (0.9)	6.9 (0.4)	–2.2 (5.6)	7.4 (7.2)	43.8 (4.9)	9.9 (1.2)
	ArO^-	–0.5 (0.6)	1.0 (0.7)	6.7 (0.4)	–2.3 (5.4)	7.0 (5.7)	43.7 (6.0)	11.0 (1.3)
	Dianionic	–0.5 (0.7)	1.3 (0.7)	6.9 (0.4)	–2.4 (5.8)	10.1 (8.4)	39.6 (6.8)	12.2 (1.2)
G^3 (stacked)	Neutral	1.1 (0.7)	–2.9 (0.7)	7.1 (0.4)	5.6 (5.8)	14.9 (5.7)	61.8 (5.7)	7.7 (0.9)
	COO^-	0.9 (0.7)	–0.6 (1.6)	7.2 (0.3)	5.7 (4.9)	11.6 (6.2)	55.8 (9.6)	8.9 (1.6)
	ArO^-	1.0 (0.7)	–1.6 (1.7)	7.3 (0.4)	5.5 (4.9)	13.3 (6.1)	58.8 (7.8)	9.2 (1.5)
	Dianionic	0.4 (1.1)	–3.4 (0.7)	7.7 (0.5)	1.5 (5.8)	11.1 (7.4)	61.4 (6.1)	7.9 (0.9)

[a]Pseudostep parameters at the lesion site were calculated using a base-step consisting of the 5′– and 3′–base pairs with respect to the OT-G adduct.

Table S11. Average values and standard deviations (in parentheses) for lesion-site pseudostep parameters[a] and minor groove dimension for DNA containing the OT-G adduct paired against G.

Position (Conformer)	Ionization State	Shift (Å)	Slide (Å)	Rise (Å)	Tilt (°)	Roll (°)	Twist (°)	Minor Groove (Å)
G^1 (Major Groove)	Neutral	0.0 (0.9)	−1.6 (1.1)	6.4 (0.4)	2.7 (5.0)	9.5 (9.4)	52.8 (7.1)	7.7 (1.5)
	COO^-	0.4 (0.7)	−3.1 (0.9)	6.7 (0.5)	3.4 (4.8)	5.6 (8.5)	51.9 (6.7)	6.8 (1.6)
	ArO^-	0.4 (0.7)	−3.6 (0.7)	6.8 (0.5)	3.6 (4.7)	5.4 (8.1)	50.5 (5.6)	6.9 (1.5)
	Dianionic	1.4 (0.9)	−0.6 (0.9)	6.5 (0.4)	0.7 (4.9)	8.0 (7.6)	54.2 (6.3)	8.2 (1.2)
G^2 (Major Groove)	Neutral	0.2 (0.7)	−3.0 (0.7)	6.7 (0.3)	3.2 (4.8)	5.4 (7.2)	59.4 (4.2)	6.9 (1.3)
	COO^-	0.6 (0.6)	−2.0 (0.8)	6.6 (0.3)	2.4 (4.9)	6.1 (6.5)	59.0 (5.4)	7.0 (1.4)
	ArO^-	0.2 (0.7)	−2.9 (0.8)	6.7 (0.3)	2.9 (4.7)	5.0 (6.6)	60.1 (4.2)	6.9 (1.3)
	Dianionic	0.9 (0.6)	−1.3 (0.9)	6.8 (0.4)	0.5 (4.8)	17.4 (6.7)	38.9 (6.4)	11.3 (1.6)
G^3 (Major Groove)	Neutral	−0.2 (0.8)	−3.2 (1.3)	6.8 (0.4)	4.5 (4.9)	2.9 (6.7)	58.6 (6.2)	5.9 (1.3)
	COO^-	1.4 (0.7)	−0.7 (0.6)	6.3 (0.4)	3.8 (4.7)	1.4 (7.7)	55.2 (4.6)	7.8 (1.4)
	ArO^-	−0.1 (0.7)	−3.4 (0.6)	6.9 (0.4)	4.5 (4.8)	3.8 (7.8)	57.7 (4.1)	6.2 (1.4)
	Dianionic	0.7 (0.9)	−1.3 (1.0)	6.4 (0.4)	4.7 (4.9)	6.4 (7.8)	54.6 (7.5)	7.6 (1.6)
G^1 (Wedge)	Neutral	0.9 (0.7)	−1.7 (1.0)	6.5 (0.4)	2.6 (5.0)	14.5 (6.8)	58.4 (7.2)	7.9 (1.1)
	COO^-	0.7 (0.8)	−1.7 (0.9)	6.6 (0.4)	2.3 (5.0)	13.9 (6.7)	58.9 (6.2)	7.5 (0.9)
	ArO^-	0.2 (0.6)	−3.1 (0.6)	6.6 (0.4)	−0.1 (4.7)	20.3 (6.4)	51.6 (4.3)	8.8 (0.9)
	Dianionic	0.6 (0.8)	−2.3 (0.9)	6.5 (0.4)	0.5 (5.1)	16.1 (6.8)	51.8 (6.5)	8.9 (1.0)
G^2 (Wedge)	Neutral	0.7 (0.9)	−1.6 (0.7)	6.7 (0.4)	3.2 (5.2)	14.0 (7.6)	60.9 (5.0)	8.5 (1.4)
	COO^-	1.3 (0.6)	−0.6 (0.7)	6.8 (0.4)	4.4 (5.0)	5.3 (6.6)	67.2 (5.1)	6.5 (1.2)
	ArO^-	0.4 (0.8)	−2.1 (0.7)	6.8 (0.4)	1.4 (4.7)	13.3 (6.7)	59.0 (4.7)	8.8 (1.1)
	Dianionic	0.0 (1.1)	−1.6 (1.0)	6.7 (0.4)	−0.8 (5.2)	9.7 (5.5)	57.5 (4.9)	8.7 (1.1)
G^3 (Wedge)	Neutral	0.6 (0.8)	−2.0 (0.7)	6.4 (0.4)	4.9 (4.7)	14.1 (6.1)	58.5 (5.4)	7.7 (1.0)
	COO^-	0.3 (0.8)	−2.3 (0.7)	6.5 (0.4)	3.6 (4.7)	15.8 (6.1)	57.1 (5.0)	8.2 (1.0)
	ArO^-	0.2 (0.9)	−2.4 (0.7)	6.5 (0.4)	2.9 (4.9)	15.2 (8.5)	55.3 (5.2)	8.6 (1.5)
	Dianionic	0.3 (0.7)	−2.6 (0.6)	6.5 (0.4)	3.0 (4.7)	16.2 (5.3)	54.9 (4.9)	8.8 (0.8)
G^1 (Stacked)	Neutral	0.7 (0.6)	−0.2 (0.6)	6.9 (0.3)	−2.3 (4.3)	13.1 (5.1)	17.5 (4.9)	10.1 (1.5)
	COO^-	1.4 (0.7)	−0.2 (0.9)	7.3 (0.4)	7.6 (6.2)	11.6 (6.4)	48.5 (8.5)	7.5 (1.4)
	ArO^-	−0.1 (0.8)	−1.1 (0.8)	7.1 (0.4)	−0.5 (5.1)	13.8 (6.3)	39.4 (7.7)	11.0 (1.0)

	Dianionic	1.4 (0.6)	0.2 (0.6)	7.3 (0.3)	6.5 (4.8)	9.4 (5.9)	42.9 (5.0)	10.2 (0.8)
G^2 (Stacked)	Neutral	0.6 (0.9)	−0.4 (1.6)	7.1 (0.4)	5.5 (6.7)	3.1 (6.3)	57.0 (10.5)	9.2 (1.7)
	COO^-	0.1 (0.9)	1.6 (1.0)	6.8 (0.4)	−1.0 (5.6)	12.1 (8.0)	34.9 (11.4)	12.7 (1.8)
	ArO^-	–	–	–	–	–	–	–
	Dianionic	−1.5 (0.7)	0.9 (0.6)	6.9 (0.4)	−1.8 (4.8)	21.0 (7.3)	26.4 (5.2)	13.9 (1.3)
G^3 (Stacked)	Neutral	1.3 (0.6)	−2.8 (0.6)	7.2 (0.3)	5.7 (4.7)	14.1 (5.9)	63.8 (4.0)	7.5 (0.8)
	COO^-	1.2 (0.6)	−3.0 (0.7)	7.2 (0.4)	5.0 (5.1)	12.9 (5.6)	63.9 (4.8)	7.7 (0.9)
	ArO^-	1.3 (0.6)	−2.5 (1.1)	7.3 (0.4)	6.0 (4.8)	13.8 (5.7)	60.8 (7.5)	8.5 (1.1)
	Dianionic	–	–	–	–	–	–	–

[a]Pseudostep parameters at the lesion site were calculated using a base-step consisting of the 5′– and 3′–base pairs with respect to the OT-G adduct.

Table S12. Occupancies (%) of the Watson-Crick hydrogen bonds of the 3′– and 5′– base pairs flanking the lesion in the stacked conformation of DNA containing OT-G paired against A.[a]

Position	Base pair	Hydrogen bond (D–A)	Stacked conformation			
			neutral	COO^-	ArO^-	dianionic
G^1	5′C:G	N4(C) – O6(G)	96.9	98.4	98.0	98.6
		N1(G) – N3(C)	99.9	99.9	99.9	100.0
		N2(G) – O2(C)	99.9	99.7	99.4	99.5
	3′G:C	N4(C) – O6(G)	98.4	99.3	98.9	99.1
		N1(G) – N3(C)	100.0	100.0	99.9	100.0
		N2(G) – O2(C)	100.0	100.0	99.9	100.0
G^2	5′G:C	N4(C) – O6(G)	98.0	98.8	97.9	98.2
		N1(G) – N3(C)	99.8	100.0	99.9	99.9
		N2(G) – O2(C)	99.8	99.9	99.8	99.9
	3′C:G	N4(C) – O6(G)	98.9	99.8	99.0	99.6
		N1(G) – N3(C)	100.0	100.0	100.0	100.0
		N2(G) – O2(C)	100.0	100.0	100.0	100.0
G^3	5′C:G	N4(C) – O6(G)	99.4	99.4	98.6	98.6
		N1(G) – N3(C)	100.0	100.0	100.0	100.0
		N2(G) – O2(C)	99.9	99.2	99.8	99.9
	3′C:G	N4(C) – O6(G)	98.7	98.3	98.6	96.4
		N1(G) – N3(C)	99.9	99.9	99.9	99.6
		N2(G) – O2(C)	99.8	99.8	100.0	99.1

[a]Hydrogen-bonding interactions were determined using a cut-off of 3.4 Å for the donor–acceptor distance and 120° for the donor–hydrogen–acceptor angle.

Table S13. Occupancies (%) of the Watson-Crick hydrogen bonds of the 3′– and 5′– base pairs flanking the lesion in the stacked conformation of DNA containing OT-G paired against T.[a]

Position	Base pair	Hydrogen bond (D–A)	Stacked conformation			
			neutral	COO^-	ArO^-	dianionic
G^1	5′C:G	N4(C) – O6(G)	98.3	98.9	98.5	99.0
		N1(G) – N3(C)	99.9	100.0	99.9	100.0
		N2(G) – O2(C)	99.8	99.6	99.4	98.4
	3′G:C	N4(C) – O6(G)	98.7	99.4	98.0	98.8
		N1(G) – N3(C)	99.9	100.0	99.9	100.0
		N2(G) – O2(C)	100.0	100.0	100.0	100.0
G^2	5′G:C	N4(C) – O6(G)	97.3	95.6	94.4	99.7
		N1(G) – N3(C)	99.3	99.8	99.9	100.0
		N2(G) – O2(C)	99.5	99.7	99.9	100.0
	3′C:G	N4(C) – O6(G)	96.3	99.3	99.2	96.5
		N1(G) – N3(C)	100.0	100.0	100.0	99.9
		N2(G) – O2(C)	99.6	100.0	100.0	99.9
G^3	5′C:G	N4(C) – O6(G)	98.3	99.2	99.1	99.4
		N1(G) – N3(C)	99.9	100.0	100.0	100.0
		N2(G) – O2(C)	99.8	99.8	99.8	100.0
	3′C:G	N4(C) – O6(G)	98.7	99.2	98.9	98.3
		N1(G) – N3(C)	99.9	100.0	100.0	99.7
		N2(G) – O2(C)	100.0	99.9	99.9	99.3

[a]Hydrogen-bonding interactions were determined using a cut-off of 3.4 Å for the donor–acceptor distance and 120° for the donor–hydrogen–acceptor angle.

Table S14. Occupancies (%) of the Watson-Crick hydrogen bonds of the 3′– and 5′– base pairs flanking the lesion in the stacked conformation of DNA containing OT-G paired against G.[a]

Position	Base pair	Hydrogen bond (D–A)	Stacked conformation			
			neutral	COO^-	ArO^-	dianionic
G^1	5′C:G	N4(C) – O6(G)	96.1	99.3	98.9	98.8
		N1(G) – N3(C)	99.6	100.0	100.0	100.0
		N2(G) – O2(C)	99.9	99.3	99.2	99.1
	3′G:C	N4(C) – O6(G)	98.7	98.3	98.2	99.3
		N1(G) – N3(C)	100.0	99.8	99.6	100.0
		N2(G) – O2(C)	100.0	100.0	100.0	99.9
G^2	5′G:C	N4(C) – O6(G)	96.8	98.9	95.3	98.3
		N1(G) – N3(C)	99.9	100.0	99.9	99.9
		N2(G) – O2(C)	99.8	99.8	99.8	99.9
	3′C:G	N4(C) – O6(G)	99.3	98.9	99.3	99.8
		N1(G) – N3(C)	100.0	100.0	99.9	100.0
		N2(G) – O2(C)	99.9	99.8	99.9	99.9
G^3	5′C:G	N4(C) – O6(G)	99.6	99.7	99.4	99.3
		N1(G) – N3(C)	100.0	100.0	100.0	100.0
		N2(G) – O2(C)	99.9	99.9	99.9	99.8
	3′C:G	N4(C) – O6(G)	99.6	99.0	98.1	97.1
		N1(G) – N3(C)	100.0	100.0	99.8	99.8
		N2(G) – O2(C)	99.8	99.9	99.9	99.7

[a]Hydrogen-bonding interactions were determined using a cut-off of 3.4 Å for the donor–acceptor distance and 120° for the donor–hydrogen–acceptor angle.

Table S15. Relative MM-PBSA free energies (kcal mol^{-1}) for different conformations of DNA containing OT-G paired against A, T or G.

Position	Ionization State	Conformation	A	T	G
G^1	Neutral	Major Groove	0.0	10.2	9.4
		Wedge	7.2	1.2	0.0
		Stacked	2.4	0.0	6.5
G^2		Major Groove	2.6	0.0	4.7
		Wedge	2.4	7.9	0.0
		Stacked	0.0	6.7	1.8
G^3		Major Groove	3.9	0.0	13.4
		Wedge	1.3	3.0	0.0
		Stacked	0.0	2.2	4.5
G^1	COO^-	Major Groove	0.0	0.0	15.2
		Wedge	13.8	2.3	0.0
		Stacked	6.1	4.8	10.9
G^2		Major Groove	0.0	0.0	14.7
		Wedge	5.5	14.3	0.0
		Stacked	0.1	7.4	19.6
G^3		Major Groove	2.7	0.0	10.7
		Wedge	0.0	1.1	0.0
		Stacked	0.6	4.9	9.0
G^1	ArO^-	Major Groove	0.0	0.0	12.3
		Wedge	8.5	1.5	0.0
		Stacked	6.8	7.2	14.0
G^2		Major Groove	3.2	0.0	12.4
		Wedge	5.9	7.4	0.0
		Stacked	0.0	10.8	–
G^3		Major Groove	0.0	0.0	10.5
		Wedge	4.6	3.8	0.0
		Stacked	11.0	8.0	20.5
G^1	Dianionic	Major Groove	0.0	0.0	7.2
		Wedge	9.4	1.1	0.0
		Stacked	8.1	8.9	21.5
G^2		Major Groove	0.0	0.0	9.3
		Wedge	10.6	0.3	0.0
		Stacked	6.3	7.6	11.1
G^3		Major Groove	0.0	4.9	14.9
		Wedge	4.1	0.0	0.0
		Stacked	11.3	10.6	–

Table S16. Hydrogen-bond occupancies (%) for the terminal G:C base pairs over the last 10 ns of the production simulation for each DNA duplex with OT-G paired against A.[a]

Position	Ionization State	Conformation	5′–G:C[b]		3′–G:C[b]	
			Hydrogen bond (D–A)	Occupancy	Hydrogen bond (D–A)	Occupancy
G^1	Neutral	Major Groove	N4(C)–O6(G)	93.8	N4(C)–O6(G)	97.3
			N1(G)–N3(C)	99.7	N1(G)–N3(C)	99.6
			N2(G)–O2(C)	99.2	N2(G)–O2(C)	99.7
		Wedge	N4(C)–O6(G)	97.7	N4(C)–O6(G)	96.8
			N1(G)–N3(C)	99.9	N1(G)–N3(C)	99.0
			N2(G)–O2(C)	99.5	N2(G)–O2(C)	99.0
		Stacked	N4(C)–O6(G)	97.7	N4(C)–O6(G)	97.8
			N1(G)–N3(C)	99.4	N1(G)–N3(C)	99.8
			N2(G)–O2(C)	99.1	N2(G)–O2(C)	99.7
	COO^-	Major Groove	N4(C)–O6(G)	91.4	N4(C)–O6(G)	97.5
			N1(G)–N3(C)	99.3	N1(G)–N3(C)	99.7
			N2(G)–O2(C)	97.9	N2(G)–O2(C)	99.7
		Wedge	N4(C)–O6(G)	96.6	N4(C)–O6(G)	92.3
			N1(G)–N3(C)	99.8	N1(G)–N3(C)	94.8
			N2(G)–O2(C)	99.2	N2(G)–O2(C)	98.7
		Stacked	N4(C)–O6(G)	97.3	N4(C)–O6(G)	97.2
			N1(G)–N3(C)	99.9	N1(G)–N3(C)	99.5
			N2(G)–O2(C)	99.5	N2(G)–O2(C)	99.6
	ArO^-	Major Groove	N4(C)–O6(G)	94.3	N4(C)–O6(G)	97.6
			N1(G)–N3(C)	99.8	N1(G)–N3(C)	99.8
			N2(G)–O2(C)	99.4	N2(G)–O2(C)	99.7
		Wedge	N4(C)–O6(G)	96.4	N4(C)–O6(G)	97.6
			N1(G)–N3(C)	99.2	N1(G)–N3(C)	99.6
			N2(G)–O2(C)	99.4	N2(G)–O2(C)	99.7
		Stacked	N4(C)–O6(G)	97.5	N4(C)–O6(G)	97.9
			N1(G)–N3(C)	99.9	N1(G)–N3(C)	99.6
			N2(G)–O2(C)	99.7	N2(G)–O2(C)	99.6
	Dianionic	Major Groove	N4(C)–O6(G)	93.3	N4(C)–O6(G)	97.6
			N1(G)–N3(C)	99.8	N1(G)–N3(C)	99.5
			N2(G)–O2(C)	99.1	N2(G)–O2(C)	99.6
		Wedge	N4(C)–O6(G)	96.9	N4(C)–O6(G)	97.9
			N1(G)–N3(C)	99.9	N1(G)–N3(C)	99.7
			N2(G)–O2(C)	99.6	N2(G)–O2(C)	99.6
		Stacked	N4(C)–O6(G)	97.1	N4(C)–O6(G)	97.3
			N1(G)–N3(C)	99.8	N1(G)–N3(C)	99.2
			N2(G)–O2(C)	99.6	N2(G)–O2(C)	99.5
G^2	Neutral	Major Groove	N4(C)–O6(G)	94.9	N4(C)–O6(G)	95.6
			N1(G)–N3(C)	95.5	N1(G)–N3(C)	97.6
			N2(G)–O2(C)	94.6	N2(G)–O2(C)	98.9
		Wedge	N4(C)–O6(G)	95.0	N4(C)–O6(G)	86.6
			N1(G)–N3(C)	99.8	N1(G)–N3(C)	88.1
			N2(G)–O2(C)	99.2	N2(G)–O2(C)	88.0
		Stacked	N4(C)–O6(G)	94.3	N4(C)–O6(G)	97.7

			N1(G)–N3(C)	98.5	N1(G)–N3(C)	99.6
			N2(G)–O2(C)	98.1	N2(G)–O2(C)	99.6
	COO^-	Major Groove	N4(C)–O6(G)	95.5	N4(C)–O6(G)	97.5
			N1(G)–N3(C)	99.9	N1(G)–N3(C)	99.8
			N2(G)–O2(C)	99.1	N2(G)–O2(C)	99.6
		Wedge	N4(C)–O6(G)	95.2	N4(C)–O6(G)	97.2
			N1(G)–N3(C)	99.7	N1(G)–N3(C)	99.7
			N2(G)–O2(C)	99.0	N2(G)–O2(C)	99.6
		Stacked	N4(C)–O6(G)	96.0	N4(C)–O6(G)	83.6
			N1(G)–N3(C)	100.0	N1(G)–N3(C)	85.7
			N2(G)–O2(C)	99.3	N2(G)–O2(C)	87.8
	ArO^-	Major Groove	N4(C)–O6(G)	95.2	N4(C)–O6(G)	97.7
			N1(G)–N3(C)	99.8	N1(G)–N3(C)	99.8
			N2(G)–O2(C)	99.2	N2(G)–O2(C)	99.1
		Wedge	N4(C)–O6(G)	95.7	N4(C)–O6(G)	97.8
			N1(G)–N3(C)	99.9	N1(G)–N3(C)	99.7
			N2(G)–O2(C)	99.2	N2(G)–O2(C)	99.6
		Stacked	N4(C)–O6(G)	96.2	N4(C)–O6(G)	97.4
			N1(G)–N3(C)	99.8	N1(G)–N3(C)	99.6
			N2(G)–O2(C)	99.1	N2(G)–O2(C)	99.7
	Dianionic	Major Groove	N4(C)–O6(G)	93.7	N4(C)–O6(G)	97.9
			N1(G)–N3(C)	99.9	N1(G)–N3(C)	99.8
			N2(G)–O2(C)	99.3	N2(G)–O2(C)	99.5
		Wedge	N4(C)–O6(G)	93.9	N4(C)–O6(G)	97.8
			N1(G)–N3(C)	99.8	N1(G)–N3(C)	99.7
			N2(G)–O2(C)	99.1	N2(G)–O2(C)	99.3
		Stacked	N4(C)–O6(G)	95.8	N4(C)–O6(G)	97.6
			N1(G)–N3(C)	99.8	N1(G)–N3(C)	99.6
			N2(G)–O2(C)	99.3	N2(G)–O2(C)	99.5
G^3	Neutral	Major Groove	N4(C)–O6(G)	96.0	N4(C)–O6(G)	97.0
			N1(G)–N3(C)	99.9	N1(G)–N3(C)	99.0
			N2(G)–O2(C)	99.5	N2(G)–O2(C)	99.7
		Wedge	N4(C)–O6(G)	96.8	N4(C)–O6(G)	97.6
			N1(G)–N3(C)	99.9	N1(G)–N3(C)	99.7
			N2(G)–O2(C)	99.4	N2(G)–O2(C)	99.7
		Stacked	N4(C)–O6(G)	95.6	N4(C)–O6(G)	97.5
			N1(G)–N3(C)	99.9	N1(G)–N3(C)	99.6
			N2(G)–O2(C)	99.3	N2(G)–O2(C)	99.5
	COO^-	Major Groove	N4(C)–O6(G)	95.9	N4(C)–O6(G)	97.0
			N1(G)–N3(C)	99.9	N1(G)–N3(C)	99.0
			N2(G)–O2(C)	99.5	N2(G)–O2(C)	99.7
		Wedge	N4(C)–O6(G)	96.0	N4(C)–O6(G)	97.8
			N1(G)–N3(C)	99.8	N1(G)–N3(C)	99.7
			N2(G)–O2(C)	99.4	N2(G)–O2(C)	99.4
		Stacked	N4(C)–O6(G)	95.4	N4(C)–O6(G)	97.4
			N1(G)–N3(C)	99.7	N1(G)–N3(C)	99.4
			N2(G)–O2(C)	99.3	N2(G)–O2(C)	99.6
	ArO^-	Major Groove	N4(C)–O6(G)	96.5	N4(C)–O6(G)	97.7

			N1(G)–N3(C)	99.9	N1(G)–N3(C)	99.7
			N2(G)–O2(C)	99.6	N2(G)–O2(C)	97.6
		Wedge	N4(C)–O6(G)	96.1	N4(C)–O6(G)	97.9
			N1(G)–N3(C)	99.8	N1(G)–N3(C)	99.5
			N2(G)–O2(C)	99.5	N2(G)–O2(C)	99.4
		Stacked	N4(C)–O6(G)	95.4	N4(C)–O6(G)	91.6
			N1(G)–N3(C)	99.9	N1(G)–N3(C)	93.5
			N2(G)–O2(C)	99.3	N2(G)–O2(C)	93.9
	Dianionic	Major Groove	N4(C)–O6(G)	94.9	N4(C)–O6(G)	97.0
			N1(G)–N3(C)	99.8	N1(G)–N3(C)	98.9
			N2(G)–O2(C)	99.1	N2(G)–O2(C)	99.6
		Wedge	N4(C)–O6(G)	96.4	N4(C)–O6(G)	97.0
			N1(G)–N3(C)	99.7	N1(G)–N3(C)	99.3
			N2(G)–O2(C)	99.4	N2(G)–O2(C)	99.5
		Stacked	N4(C)–O6(G)	95.3	N4(C)–O6(G)	97.3
			N1(G)–N3(C)	99.7	N1(G)–N3(C)	99.4
			N2(G)–O2(C)	99.3	N2(G)–O2(C)	99.7

[a]Hydrogen-bonding interactions were determined using a cut-off of 3.4 Å for the donor–acceptor distance and 120° for the donor–hydrogen–acceptor angle. [b]5′– and 3′–G:C refer to the base pair at the 5′ and 3′ terminal ends with respect to the damaged nucleotide, respectively.

Table S17. Hydrogen-bond occupancies (%) for the terminal G:C base pairs over the last 10 ns of the production simulation for each DNA duplex with OT-G paired against T.[a]

Position	Ionization state	Conformation	5′–G:C [b]		3′–G:C [b]	
			Hydrogen bond (D–A)	Occupancy	Hydrogen bond (D–A)	Occupancy
G[1]	Neutral	Major Groove	N4(C)–O6(G)	97.2	N4(C)–O6(G)	96.6
			N1(G)–N3(C)	99.9	N1(G)–N3(C)	98.9
			N2(G)–O2(C)	99.2	N2(G)–O2(C)	99.6
		Wedge	N4(C)–O6(G)	96.1	N4(C)–O6(G)	97.7
			N1(G)–N3(C)	99.9	N1(G)–N3(C)	99.7
			N2(G)–O2(C)	99.3	N2(G)–O2(C)	99.7
		Stacked	N4(C)–O6(G)	97.6	N4(C)–O6(G)	96.5
			N1(G)–N3(C)	99.9	N1(G)–N3(C)	98.8
			N2(G)–O2(C)	99.6	N2(G)–O2(C)	99.6
	COO^-	Major Groove	N4(C)–O6(G)	91.3	N4(C)–O6(G)	97.7
			N1(G)–N3(C)	99.8	N1(G)–N3(C)	99.7
			N2(G)–O2(C)	98.9	N2(G)–O2(C)	99.5
		Wedge	N4(C)–O6(G)	95.3	N4(C)–O6(G)	96.9
			N1(G)–N3(C)	99.9	N1(G)–N3(C)	99.0
			N2(G)–O2(C)	99.2	N2(G)–O2(C)	99.5
		Stacked	N4(C)–O6(G)	97.5	N4(C)–O6(G)	97.4
			N1(G)–N3(C)	99.8	N1(G)–N3(C)	99.4
			N2(G)–O2(C)	99.4	N2(G)–O2(C)	99.5
	ArO^-	Major Groove	N4(C)–O6(G)	95.5	N4(C)–O6(G)	97.6
			N1(G)–N3(C)	99.5	N1(G)–N3(C)	99.5
			N2(G)–O2(C)	98.5	N2(G)–O2(C)	99.4
		Wedge	N4(C)–O6(G)	93.6	N4(C)–O6(G)	98.0
			N1(G)–N3(C)	99.3	N1(G)–N3(C)	99.8
			N2(G)–O2(C)	98.8	N2(G)–O2(C)	99.6
		Stacked	N4(C)–O6(G)	97.9	N4(C)–O6(G)	97.9
			N1(G)–N3(C)	99.9	N1(G)–N3(C)	99.7
			N2(G)–O2(C)	99.6	N2(G)–O2(C)	99.7
	Dianionic	Major Groove	N4(C)–O6(G)	89.1	N4(C)–O6(G)	97.6
			N1(G)–N3(C)	99.7	N1(G)–N3(C)	99.6
			N2(G)–O2(C)	98.3	N2(G)–O2(C)	99.6
		Wedge	N4(C)–O6(G)	95.6	N4(C)–O6(G)	97.7
			N1(G)–N3(C)	99.9	N1(G)–N3(C)	99.6
			N2(G)–O2(C)	99.4	N2(G)–O2(C)	99.5
		Stacked	N4(C)–O6(G)	97.5	N4(C)–O6(G)	97.5
			N1(G)–N3(C)	99.9	N1(G)–N3(C)	99.3
			N2(G)–O2(C)	99.4	N2(G)–O2(C)	99.6
G[2]	Neutral	Major Groove	N4(C)–O6(G)	95.6	N4(C)–O6(G)	97.3
			N1(G)–N3(C)	99.9	N1(G)–N3(C)	99.1
			N2(G)–O2(C)	99.5	N2(G)–O2(C)	99.7
		Wedge	N4(C)–O6(G)	94.8	N4(C)–O6(G)	81.2
			N1(G)–N3(C)	99.9	N1(G)–N3(C)	92.2
			N2(G)–O2(C)	99.2	N2(G)–O2(C)	87.2
		Stacked	N4(C)–O6(G)	95.0	N4(C)–O6(G)	95.0

			N1(G)–N3(C)	99.8	N1(G)–N3(C)	99.8
			N2(G)–O2(C)	98.9	N2(G)–O2(C)	98.9
	COO^-	Major Groove	N4(C)–O6(G)	94.0	N4(C)–O6(G)	87.0
			N1(G)–N3(C)	99.4	N1(G)–N3(C)	89.7
			N2(G)–O2(C)	98.8	N2(G)–O2(C)	93.7
		Wedge	N4(C)–O6(G)	95.2	N4(C)–O6(G)	96.8
			N1(G)–N3(C)	99.7	N1(G)–N3(C)	98.9
			N2(G)–O2(C)	99.4	N2(G)–O2(C)	99.4
		Stacked	N4(C)–O6(G)	95.0	N4(C)–O6(G)	97.3
			N1(G)–N3(C)	99.8	N1(G)–N3(C)	99.6
			N2(G)–O2(C)	98.9	N2(G)–O2(C)	99.7
	ArO^-	Major Groove	N4(C)–O6(G)	96.9	N4(C)–O6(G)	97.2
			N1(G)–N3(C)	99.8	N1(G)–N3(C)	99.4
			N2(G)–O2(C)	99.2	N2(G)–O2(C)	99.7
		Wedge	N4(C)–O6(G)	95.9	N4(C)–O6(G)	95.7
			N1(G)–N3(C)	99.7	N1(G)–N3(C)	97.9
			N2(G)–O2(C)	99.3	N2(G)–O2(C)	99.1
		Stacked	N4(C)–O6(G)	97.2	N4(C)–O6(G)	97.1
			N1(G)–N3(C)	99.9	N1(G)–N3(C)	99.3
			N2(G)–O2(C)	99.3	N2(G)–O2(C)	99.5
	Dianionic	Major Groove	N4(C)–O6(G)	91.9	N4(C)–O6(G)	97.3
			N1(G)–N3(C)	99.6	N1(G)–N3(C)	99.0
			N2(G)–O2(C)	98.9	N2(G)–O2(C)	99.3
		Wedge	N4(C)–O6(G)	95.2	N4(C)–O6(G)	97.9
			N1(G)–N3(C)	99.9	N1(G)–N3(C)	99.7
			N2(G)–O2(C)	99.2	N2(G)–O2(C)	99.7
		Stacked	N4(C)–O6(G)	96.0	N4(C)–O6(G)	97.8
			N1(G)–N3(C)	99.9	N1(G)–N3(C)	99.6
			N2(G)–O2(C)	99.2	N2(G)–O2(C)	99.6
G^3	Neutral	Major Groove	N4(C)–O6(G)	95.6	N4(C)–O6(G)	97.5
			N1(G)–N3(C)	99.8	N1(G)–N3(C)	99.5
			N2(G)–O2(C)	99.2	N2(G)–O2(C)	99.3
		Wedge	N4(C)–O6(G)	95.4	N4(C)–O6(G)	97.6
			N1(G)–N3(C)	99.9	N1(G)–N3(C)	99.7
			N2(G)–O2(C)	99.3	N2(G)–O2(C)	99.6
		Stacked	N4(C)–O6(G)	95.6	N4(C)–O6(G)	97.4
			N1(G)–N3(C)	99.7	N1(G)–N3(C)	99.5
			N2(G)–O2(C)	99.3	N2(G)–O2(C)	99.5
	COO^-	Major Groove	N4(C)–O6(G)	95.6	N4(C)–O6(G)	97.4
			N1(G)–N3(C)	99.4	N1(G)–N3(C)	99.3
			N2(G)–O2(C)	99.8	N2(G)–O2(C)	99.4
		Wedge	N4(C)–O6(G)	95.6	N4(C)–O6(G)	96.7
			N1(G)–N3(C)	100.0	N1(G)–N3(C)	98.9
			N2(G)–O2(C)	99.4	N2(G)–O2(C)	99.5
		Stacked	N4(C)–O6(G)	94.4	N4(C)–O6(G)	95.0
			N1(G)–N3(C)	99.8	N1(G)–N3(C)	97.2
			N2(G)–O2(C)	99.3	N2(G)–O2(C)	99.6
	ArO^-	Major Groove	N4(C)–O6(G)	94.9	N4(C)–O6(G)	98.0

			N1(G)–N3(C)	98.8	N1(G)–N3(C)	99.7
			N2(G)–O2(C)	99.4	N2(G)–O2(C)	99.6
		Wedge	N4(C)–O6(G)	94.0	N4(C)–O6(G)	98.0
			N1(G)–N3(C)	99.4	N1(G)–N3(C)	99.7
			N2(G)–O2(C)	98.8	N2(G)–O2(C)	99.6
		Stacked	N4(C)–O6(G)	93.5	N4(C)–O6(G)	97.5
			N1(G)–N3(C)	99.4	N1(G)–N3(C)	99.5
			N2(G)–O2(C)	98.3	N2(G)–O2(C)	99.7
	Dianionic	Major Groove	N4(C)–O6(G)	87.9	N4(C)–O6(G)	98.0
			N1(G)–N3(C)	91.0	N1(G)–N3(C)	99.9
			N2(G)–O2(C)	91.2	N2(G)–O2(C)	99.7
		Wedge	N4(C)–O6(G)	83.9	N4(C)–O6(G)	97.4
			N1(G)–N3(C)	97.4	N1(G)–N3(C)	99.2
			N2(G)–O2(C)	93.7	N2(G)–O2(C)	99.6
		Stacked	N4(C)–O6(G)	95.2	N4(C)–O6(G)	97.7
			N1(G)–N3(C)	99.1	N1(G)–N3(C)	99.5
			N2(G)–O2(C)	98.5	N2(G)–O2(C)	99.7

[a]Hydrogen-bonding interactions were determined using a cut-off of 3.4 Å for the donor–acceptor distance and 120° for the donor–hydrogen–acceptor angle. [b]5′– and 3′–G:C refer to the base pair at the 5′ and 3′ terminal ends with respect to the damaged nucleotide, respectively.

Table S18. Hydrogen-bond occupancies (%) for the terminal G:C base pairs over the last 10 ns of the production simulation for each DNA duplex with OT-G paired against G.[a]

Position	Ionization state	Conformation	5′–G:C[b]		3′–G:C[b]	
			Hydrogen bond (D–A)	Occupancy	Hydrogen bond (D–A)	Occupancy
G[1]	Neutral	Major Groove	N4(C)–O6(G)	95.4	N4(C)–O6(G)	97.0
			N1(G)–N3(C)	99.8	N1(G)–N3(C)	99.5
			N2(G)–O2(C)	99.7	N2(G)–O2(C)	99.5
		Wedge	N4(C)–O6(G)	96.1	N4(C)–O6(G)	96.9
			N1(G)–N3(C)	99.9	N1(G)–N3(C)	98.9
			N2(G)–O2(C)	99.5	N2(G)–O2(C)	99.5
		Stacked	N4(C)–O6(G)	97.6	N4(C)–O6(G)	97.6
			N1(G)–N3(C)	99.9	N1(G)–N3(C)	99.7
			N2(G)–O2(C)	99.5	N2(G)–O2(C)	99.6
	COO^-	Major Groove	N4(C)–O6(G)	96.3	N4(C)–O6(G)	97.8
			N1(G)–N3(C)	99.7	N1(G)–N3(C)	99.6
			N2(G)–O2(C)	99.3	N2(G)–O2(C)	99.6
		Wedge	N4(C)–O6(G)	88.5	N4(C)–O6(G)	97.5
			N1(G)–N3(C)	92.4	N1(G)–N3(C)	99.4
			N2(G)–O2(C)	91.4	N2(G)–O2(C)	99.6
		Stacked	N4(C)–O6(G)	97.5	N4(C)–O6(G)	97.9
			N1(G)–N3(C)	99.9	N1(G)–N3(C)	99.7
			N2(G)–O2(C)	99.5	N2(G)–O2(C)	99.7
	ArO^-	Major Groove	N4(C)–O6(G)	97.3	N4(C)–O6(G)	97.6
			N1(G)–N3(C)	99.8	N1(G)–N3(C)	99.6
			N2(G)–O2(C)	99.5	N2(G)–O2(C)	99.5
		Wedge	N4(C)–O6(G)	96.7	N4(C)–O6(G)	97.3
			N1(G)–N3(C)	99.0	N1(G)–N3(C)	99.1
			N2(G)–O2(C)	98.3	N2(G)–O2(C)	99.5
		Stacked	N4(C)–O6(G)	95.2	N4(C)–O6(G)	97.8
			N1(G)–N3(C)	99.5	N1(G)–N3(C)	99.8
			N2(G)–O2(C)	97.1	N2(G)–O2(C)	99.6
	Dianionic	Major Groove	N4(C)–O6(G)	96.1	N4(C)–O6(G)	97.8
			N1(G)–N3(C)	99.8	N1(G)–N3(C)	99.6
			N2(G)–O2(C)	99.4	N2(G)–O2(C)	97.8
		Wedge	N4(C)–O6(G)	96.1	N4(C)–O6(G)	97.4
			N1(G)–N3(C)	94.3	N1(G)–N3(C)	99.5
			N2(G)–O2(C)	93.9	N2(G)–O2(C)	99.4
		Stacked	N4(C)–O6(G)	96.9	N4(C)–O6(G)	96.9
			N1(G)–N3(C)	99.7	N1(G)–N3(C)	98.9
			N2(G)–O2(C)	99.3	N2(G)–O2(C)	99.4
G[2]	Neutral	Major Groove	N4(C)–O6(G)	95.8	N4(C)–O6(G)	94.8
			N1(G)–N3(C)	98.6	N1(G)–N3(C)	96.4
			N2(G)–O2(C)	98.1	N2(G)–O2(C)	98.8
		Wedge	N4(C)–O6(G)	95.5	N4(C)–O6(G)	97.4
			N1(G)–N3(C)	99.9	N1(G)–N3(C)	99.5
			N2(G)–O2(C)	99.2	N2(G)–O2(C)	99.4
		Stacked	N4(C)–O6(G)	97.0	N4(C)–O6(G)	97.8

			N1(G)–N3(C)	99.9	N1(G)–N3(C)	99.6
			N2(G)–O2(C)	99.5	N2(G)–O2(C)	99.6
	COO^-	Major Groove	N4(C)–O6(G)	95.2	N4(C)–O6(G)	97.6
			N1(G)–N3(C)	99.7	N1(G)–N3(C)	99.5
			N2(G)–O2(C)	99.0	N2(G)–O2(C)	99.6
		Wedge	N4(C)–O6(G)	96.6	N4(C)–O6(G)	97.7
			N1(G)–N3(C)	99.2	N1(G)–N3(C)	99.5
			N2(G)–O2(C)	98.4	N2(G)–O2(C)	99.5
		Stacked	N4(C)–O6(G)	95.4	N4(C)–O6(G)	97.9
			N1(G)–N3(C)	99.8	N1(G)–N3(C)	99.8
			N2(G)–O2(C)	99.3	N2(G)–O2(C)	99.7
	ArO^-	Major Groove	N4(C)–O6(G)	95.2	N4(C)–O6(G)	97.6
			N1(G)–N3(C)	99.7	N1(G)–N3(C)	99.5
			N2(G)–O2(C)	99.0	N2(G)–O2(C)	99.6
		Wedge	N4(C)–O6(G)	96.3	N4(C)–O6(G)	98.0
			N1(G)–N3(C)	99.6	N1(G)–N3(C)	99.7
			N2(G)–O2(C)	99.0	N2(G)–O2(C)	99.7
	Dianionic	Major Groove	N4(C)–O6(G)	96.4	N4(C)–O6(G)	97.3
			N1(G)–N3(C)	99.6	N1(G)–N3(C)	99.5
			N2(G)–O2(C)	99.5	N2(G)–O2(C)	99.5
		Wedge	N4(C)–O6(G)	96.1	N4(C)–O6(G)	97.3
			N1(G)–N3(C)	99.9	N1(G)–N3(C)	99.5
			N2(G)–O2(C)	99.3	N2(G)–O2(C)	99.4
		Stacked	N4(C)–O6(G)	96.0	N4(C)–O6(G)	97.5
			N1(G)–N3(C)	99.5	N1(G)–N3(C)	99.5
			N2(G)–O2(C)	99.3	N2(G)–O2(C)	99.4
G^3	Neutral	Major Groove	N4(C)–O6(G)	96.1	N4(C)–O6(G)	97.4
			N1(G)–N3(C)	99.9	N1(G)–N3(C)	99.5
			N2(G)–O2(C)	99.3	N2(G)–O2(C)	99.6
		Wedge	N4(C)–O6(G)	96.3	N4(C)–O6(G)	98.0
			N1(G)–N3(C)	99.7	N1(G)–N3(C)	99.7
			N2(G)–O2(C)	99.6	N2(G)–O2(C)	99.7
		Stacked	N4(C)–O6(G)	95.6	N4(C)–O6(G)	97.3
			N1(G)–N3(C)	99.8	N1(G)–N3(C)	99.3
			N2(G)–O2(C)	99.3	N2(G)–O2(C)	99.6
	COO^-	Major Groove	N4(C)–O6(G)	96.0	N4(C)–O6(G)	97.4
			N1(G)–N3(C)	99.9	N1(G)–N3(C)	99.6
			N2(G)–O2(C)	99.3	N2(G)–O2(C)	99.7
		Wedge	N4(C)–O6(G)	95.1	N4(C)–O6(G)	98.0
			N1(G)–N3(C)	99.9	N1(G)–N3(C)	99.8
			N2(G)–O2(C)	99.3	N2(G)–O2(C)	99.6
		Stacked	N4(C)–O6(G)	95.2	N4(C)–O6(G)	97.8
			N1(G)–N3(C)	99.8	N1(G)–N3(C)	99.8
			N2(G)–O2(C)	99.4	N2(G)–O2(C)	99.7
	ArO^-	Major Groove	N4(C)–O6(G)	96.6	N4(C)–O6(G)	95.9
			N1(G)–N3(C)	99.5	N1(G)–N3(C)	98.2
			N2(G)–O2(C)	99.5	N2(G)–O2(C)	99.6
		Wedge	N4(C)–O6(G)	96.4	N4(C)–O6(G)	97.3

			N1(G)–N3(C)	99.8	N1(G)–N3(C)	99.4
			N2(G)–O2(C)	99.5	N2(G)–O2(C)	99.2
		Stacked	N4(C)–O6(G)	70.3	N4(C)–O6(G)	85.2
			N1(G)–N3(C)	78.5	N1(G)–N3(C)	87.2
			N2(G)–O2(C)	81.0	N2(G)–O2(C)	93.4
	Dianionic	Major Groove	N4(C)–O6(G)	96.2	N4(C)–O6(G)	96.2
			N1(G)–N3(C)	99.9	N1(G)–N3(C)	98.7
			N2(G)–O2(C)	99.5	N2(G)–O2(C)	99.4
		Wedge	N4(C)–O6(G)	96.4	N4(C)–O6(G)	92.7
			N1(G)–N3(C)	99.6	N1(G)–N3(C)	95.3
			N2(G)–O2(C)	99.1	N2(G)–O2(C)	98.5

[a]Hydrogen-bonding interactions were determined using a cut-off of 3.4 Å for the donor–acceptor distance and 120° for the donor–hydrogen–acceptor angle. [b]5′– and 3′–G:C refer to the base pair at the 5′ and 3′ terminal ends with respect to the damaged nucleotide, respectively.

Table S19. Partial charges of the neutral OT-G adduct generated using the RED program.

P	P	0	1	131072	1	15	1.1706
O	OS	0	1	131072	2	8	-0.4973
O1	O2	0	1	131072	3	8	-0.7693
O2	O2	0	1	131072	4	8	-0.7693
O3	OS	0	1	131072	5	8	-0.544
C5*	CI	0	1	131072	6	6	-0.0335
H5*1	H1	0	1	131072	7	1	0.0862
H5*2	H1	0	1	131072	8	1	0.0862
C4*	CT	0	1	131072	9	6	0.1607
H4*	H1	0	1	131072	10	1	0.0844
O4*	OS	0	1	131072	11	8	-0.3953
C1*	CT	0	1	131072	12	6	0.1501
H1*	H2	0	1	131072	13	1	0.035
C3*	CT	0	1	131072	14	6	0.173
H3*	H1	0	1	131072	15	1	0.0625
C2*	CT	0	1	131072	16	6	-0.0039
H2*1	HC	0	1	131072	17	1	0.0336
H2*2	HC	0	1	131072	18	1	0.0336
CG	CA	0	1	131072	19	6	0.0072
CD1	CA	0	1	131072	20	6	-0.0855
HD1	HA	0	1	131072	21	1	0.1389
CE1	CA	0	1	131072	22	6	-0.1933
HE1	HA	0	1	131072	23	1	0.1489
CZ	CA	0	1	131072	24	6	-0.1123
HZ	HA	0	1	131072	25	1	0.1356
CE2	CA	0	1	131072	26	6	-0.1748
HE2	HA	0	1	131072	27	1	0.1477
CD2	CA	0	1	131072	28	6	-0.1147
HD2	HA	0	1	131072	29	1	0.1101
CB	CT	0	1	131072	30	6	-0.101
HB1	HC	0	1	131072	31	1	0.0629
HB2	HC	0	1	131072	32	1	0.0629
CA	CT	0	1	131072	33	6	-0.0087
HA	H1	0	1	131072	34	1	0.0906
N	N	0	1	131072	35	7	-0.2329
H	H	0	1	131072	36	1	0.2161
C	C	0	1	131072	37	6	0.6594
O5	O	0	1	131072	38	8	-0.5178
OXT	OH	0	1	131072	39	8	-0.6158
HXT	HO	0	1	131072	40	1	0.4385
C6	C	0	1	131072	41	6	0.4301
O6	O	0	1	131072	42	8	-0.5901

C7	CA	0	1	131072	43	6	-0.0215
C8	CA	0	1	131072	44	6	0.0799
C9	CA	0	1	131072	45	6	-0.0174
H6	HA	0	1	131072	46	1	0.1589
C10	CA	0	1	131072	47	6	-0.0876
C11	CA	0	1	131072	48	6	-0.0181
C12	CA	0	1	131072	49	6	-0.085
C13	CT	0	1	131072	50	6	-0.0203
H7	HC	0	1	131072	51	1	0.0665
H8	HC	0	1	131072	52	1	0.0665
C14	CT	0	1	131072	53	6	0.3187
H9	H1	0	1	131072	54	1	0.0234
O7	OH	0	1	131072	55	8	-0.4558
H10	HO	0	1	131072	56	1	0.4378
C15	C	0	1	131072	57	6	0.7249
O8	O	0	1	131072	58	8	-0.5964
O9	OS	0	1	131072	59	8	-0.4341
C16	CK	0	1	131072	60	6	0.1759
N1	N*	0	1	131072	61	7	0.0358
N2	NB	0	1	131072	62	7	-0.444
C17	CB	0	1	131072	63	6	0.1588
C18	CB	0	1	131072	64	6	0.0765
N3	NC	0	1	131072	65	7	-0.4179
C19	C	0	1	131072	66	6	0.4743
C20	CA	0	1	131072	67	6	0.5064
O10	O	0	1	131072	68	8	-0.538
N4	NA	0	1	131072	69	7	-0.4021
H11	H	0	1	131072	70	1	0.3382
N5	N2	0	1	131072	71	7	-0.8147
H12	H	0	1	131072	72	1	0.38
H13	H	0	1	131072	73	1	0.38
C21	CT	0	1	131072	74	6	-0.2576
H14	HC	0	1	131072	75	1	0.0811
H15	HC	0	1	131072	76	1	0.0811
H16	HC	0	1	131072	77	1	0.0811

Table S20. Partial charges of the monoanionic (carboxylic group ionized) OT-G adduct generated using the RED program**.**

P	P	0	1	131072	1	15	1.1658
O	OS	0	1	131072	2	8	-0.5093
O1	O2	0	1	131072	3	8	-0.7674
O2	O2	0	1	131072	4	8	-0.7674
O3	OS	0	1	131072	5	8	-0.5408
C5*	CI	0	1	131072	6	6	0.0116
H5*1	H1	0	1	131072	7	1	0.073
H5*2	H1	0	1	131072	8	1	0.073
C4*	CT	0	1	131072	9	6	0.1496
H4*	H1	0	1	131072	10	1	0.1153
O4*	OS	0	1	131072	11	8	-0.4216
C1*	CT	0	1	131072	12	6	-0.0633
H1*	H2	0	1	131072	13	1	0.2083
C3*	CT	0	1	131072	14	6	0.1291
H3*	H1	0	1	131072	15	1	0.0747
C2*	CT	0	1	131072	16	6	-0.0717
H2*1	HC	0	1	131072	17	1	0.0491
H2*2	HC	0	1	131072	18	1	0.0491
CG	CA	0	1	131072	19	6	0.0155
CD1	CA	0	1	131072	20	6	-0.0912
HD1	HA	0	1	131072	21	1	0.1453
CE1	CA	0	1	131072	22	6	-0.1824
HE1	HA	0	1	131072	23	1	0.1271
CZ	CA	0	1	131072	24	6	-0.1216
HZ	HA	0	1	131072	25	1	0.1167
CE2	CA	0	1	131072	26	6	-0.1793
HE2	HA	0	1	131072	27	1	0.1342
CD2	CA	0	1	131072	28	6	-0.186
HD2	HA	0	1	131072	29	1	0.1598
CB	CT	0	1	131072	30	6	-0.0585
HB1	HC	0	1	131072	31	1	0.0425
HB2	HC	0	1	131072	32	1	0.0425
CA	CT	0	1	131072	33	6	0.0324
HA	H1	0	1	131072	34	1	0.0614
N	N	0	1	131072	35	7	-0.2321
H	H	0	1	131072	36	1	0.1873
C	C	0	1	131072	37	6	0.68
O5	O2	0	1	131072	38	8	-0.6897
OXT	O2	0	1	131072	39	8	-0.6865
C6	C	0	1	131072	40	6	0.4082

O6	O	0	1	131072	41	8	-0.5622
C7	CA	0	1	131072	42	6	-0.0299
C8	CA	0	1	131072	43	6	0.2541
C9	CA	0	1	131072	44	6	-0.2864
H6	HA	0	1	131072	45	1	0.227
C10	CA	0	1	131072	46	6	-0.1049
C11	CA	0	1	131072	47	6	-0.0382
C12	CA	0	1	131072	48	6	-0.0806
C13	CT	0	1	131072	49	6	-0.0313
H7	HC	0	1	131072	50	1	0.0659
H8	HC	0	1	131072	51	1	0.0659
C14	CT	0	1	131072	52	6	0.3359
H9	H1	0	1	131072	53	1	0.0019
O7	OH	0	1	131072	54	8	-0.5191
H10	HO	0	1	131072	55	1	0.4278
C15	C	0	1	131072	56	6	0.7597
O8	O	0	1	131072	57	8	-0.5604
O9	OS	0	1	131072	58	8	-0.4985
C16	CK	0	1	131072	59	6	0.3168
N1	N*	0	1	131072	60	7	0.0364
N2	NB	0	1	131072	61	7	-0.5346
C17	CB	0	1	131072	62	6	0.1063
C18	CB	0	1	131072	63	6	0.1361
N3	NC	0	1	131072	64	7	-0.375
C19	C	0	1	131072	65	6	0.4291
C20	CA	0	1	131072	66	6	0.4623
O10	O	0	1	131072	67	8	-0.5465
N4	NA	0	1	131072	68	7	-0.3501
H11	H	0	1	131072	69	1	0.3233
N5	N2	0	1	131072	70	7	-0.8095
H12	H	0	1	131072	71	1	0.3664
H13	H	0	1	131072	72	1	0.3664
C21	CT	0	1	131072	73	6	-0.2181
H14	HC	0	1	131072	74	1	0.0605
H15	HC	0	1	131072	75	1	0.0605
H16	HC	0	1	131072	76	1	0.0605

Table S21. Partial charges of the dianionic (phenolic group ionized) OT-G adduct generated using the RED program**.**

P	P	0	1	131072	1	15	1.1662
O	OS	0	1	131072	2	8	-0.4929
O1	O2	0	1	131072	3	8	-0.7684
O2	O2	0	1	131072	4	8	-0.7684
O3	OS	0	1	131072	5	8	-0.5366
C5*	CI	0	1	131072	6	6	-0.0143
H5*1	H1	0	1	131072	7	1	0.081
H5*2	H1	0	1	131072	8	1	0.081
C4*	CT	0	1	131072	9	6	0.1285
H4*	H1	0	1	131072	10	1	0.096
O4*	OS	0	1	131072	11	8	-0.395
C1*	CT	0	1	131072	12	6	-0.0531
H1*	H2	0	1	131072	13	1	0.0814
C3*	CT	0	1	131072	14	6	0.1593
H3*	H1	0	1	131072	15	1	0.0689
C2*	CT	0	1	131072	16	6	-0.02
H2*1	HC	0	1	131072	17	1	0.0386
H2*2	HC	0	1	131072	18	1	0.0386
CG	CA	0	1	131072	19	6	-0.0086
CD1	CA	0	1	131072	20	6	-0.0927
HD1	HA	0	1	131072	21	1	0.135
CE1	CA	0	1	131072	22	6	-0.2113
HE1	HA	0	1	131072	23	1	0.1304
CZ	CA	0	1	131072	24	6	-0.1021
HZ	HA	0	1	131072	25	1	0.1141
CE2	CA	0	1	131072	26	6	-0.1953
HE2	HA	0	1	131072	27	1	0.155
CD2	CA	0	1	131072	28	6	-0.1014
HD2	HA	0	1	131072	29	1	0.1327
CB	CT	0	1	131072	30	6	-0.0626
HB1	HC	0	1	131072	31	1	0.0348
HB2	HC	0	1	131072	32	1	0.0348
CA	CT	0	1	131072	33	6	0.0879
HA	H1	0	1	131072	34	1	0.0448
N	N	0	1	131072	35	7	-0.3014
H	H	0	1	131072	36	1	0.2226
C	C	0	1	131072	37	6	0.6695
OXT	O	0	1	131072	38	8	-0.5598
O5	OH	0	1	131072	39	8	-0.6407
H6	HO	0	1	131072	40	1	0.4443
C6	C	0	1	131072	41	6	0.4661

O6	O	0	1	131072	42	8	-0.6567
C7	CA	0	1	131072	43	6	-0.1179
C8	C	0	1	131072	44	6	0.2048
C9	CA	0	1	131072	45	6	-0.0865
H7	HA	0	1	131072	46	1	0.1914
C10	CA	0	1	131072	47	6	-0.1234
C11	CA	0	1	131072	48	6	-0.0158
C12	CA	0	1	131072	49	6	-0.1037
C13	CT	0	1	131072	50	6	0.001
H8	HC	0	1	131072	51	1	0.0408
H9	HC	0	1	131072	52	1	0.0408
C14	CT	0	1	131072	53	6	0.3846
H10	H1	0	1	131072	54	1	-0.0062
O7	O	0	1	131072	55	8	-0.4954
C15	C	0	1	131072	56	6	0.7011
O8	O	0	1	131072	57	8	-0.5637
O9	OS	0	1	131072	58	8	-0.5086
C16	CK	0	1	131072	59	6	0.0569
N1	N*	0	1	131072	60	7	0.3077
N2	NB	0	1	131072	61	7	-0.4552
C17	CB	0	1	131072	62	6	0.0574
C18	CB	0	1	131072	63	6	0.0802
N3	NC	0	1	131072	64	7	-0.4424
C19	C	0	1	131072	65	6	0.5276
C20	CA	0	1	131072	66	6	0.579
O10	O	0	1	131072	67	8	-0.5723
N4	NA	0	1	131072	68	7	-0.4711
H11	H	0	1	131072	69	1	0.3423
N5	N2	0	1	131072	70	7	-0.844
H12	H	0	1	131072	71	1	0.3672
H13	H	0	1	131072	72	1	0.3672
C21	CT	0	1	131072	73	6	-0.2371
H14	HC	0	1	131072	74	1	0.0544
H15	HC	0	1	131072	75	1	0.0544
H16	HC	0	1	131072	76	1	0.0544

Table S22. Partial charges of the dianionic (carboxylic and phenolic group ionized) OT-G **a**dduct generated using the RED program**.**

P	P	0	1	131072	1	15	1.165
O	OS	0	1	131072	2	8	-0.5277
O1	O2	0	1	131072	3	8	-0.7663
O2	O2	0	1	131072	4	8	-0.7663
O3	OS	0	1	131072	5	8	-0.545
C5*	CI	0	1	131072	6	6	-0.0142
H5*1	H1	0	1	131072	7	1	0.0857
H5*2	H1	0	1	131072	8	1	0.0857
C4*	CT	0	1	131072	9	6	0.1445
H4*	H1	0	1	131072	10	1	0.1083
O4*	OS	0	1	131072	11	8	-0.413
C1*	CT	0	1	131072	12	6	-0.0755
H1*	H2	0	1	131072	13	1	0.1369
C3*	CT	0	1	131072	14	6	0.1425
H3*	H1	0	1	131072	15	1	0.0885
C2*	CT	0	1	131072	16	6	-0.0859
H2*1	HC	0	1	131072	17	1	0.0548
H2*2	HC	0	1	131072	18	1	0.0548
CG	CA	0	1	131072	19	6	-0.0311
CD1	CA	0	1	131072	20	6	-0.1002
HD1	HA	0	1	131072	21	1	0.1134
CE1	CA	0	1	131072	22	6	-0.2011
HE1	HA	0	1	131072	23	1	0.1168
CZ	CA	0	1	131072	24	6	-0.1414
HZ	HA	0	1	131072	25	1	0.1071
CE2	CA	0	1	131072	26	6	-0.169
HE2	HA	0	1	131072	27	1	0.1256
CD2	CA	0	1	131072	28	6	-0.1089
HD2	HA	0	1	131072	29	1	0.146
CB	CT	0	1	131072	30	6	-0.1223
HB1	HC	0	1	131072	31	1	0.0769
HB2	HC	0	1	131072	32	1	0.0769
CA	CT	0	1	131072	33	6	0.0837
HA	H1	0	1	131072	34	1	0.0269
N	N	0	1	131072	35	7	-0.1664
H	H	0	1	131072	36	1	0.2006
C	C	0	1	131072	37	6	0.7687
O5	O2	0	1	131072	38	8	-0.7572
OXT	O2	0	1	131072	39	8	-0.7822
C6	C	0	1	131072	40	6	0.2756
O6	O	0	1	131072	41	8	-0.5437

C7	CA	0	1	131072	42	6	-0.0213
C8	C	0	1	131072	43	6	0.329
C9	CA	0	1	131072	44	6	-0.1793
H6	HA	0	1	131072	45	1	0.1654
C10	CA	0	1	131072	46	6	-0.2033
C11	CA	0	1	131072	47	6	-0.0352
C12	CA	0	1	131072	48	6	-0.1103
C13	CT	0	1	131072	49	6	-0.0097
H7	HC	0	1	131072	50	1	0.0437
H8	HC	0	1	131072	51	1	0.0437
C14	CT	0	1	131072	52	6	0.3777
H9	H1	0	1	131072	53	1	0.001
O7	O	0	1	131072	54	8	-0.5876
C15	C	0	1	131072	55	6	0.731
O8	O	0	1	131072	56	8	-0.5924
O9	OS	0	1	131072	57	8	-0.5076
C16	CK	0	1	131072	58	6	0.2933
N1	N*	0	1	131072	59	7	0.1072
N2	NB	0	1	131072	60	7	-0.5975
C17	CB	0	1	131072	61	6	0.1587
C18	CB	0	1	131072	62	6	0.1077
N3	NC	0	1	131072	63	7	-0.567
C19	C	0	1	131072	64	6	0.5549
C20	CA	0	1	131072	65	6	0.715
O10	O	0	1	131072	66	8	-0.5956
N4	NA	0	1	131072	67	7	-0.5721
H10	H	0	1	131072	68	1	0.3543
N5	N2	0	1	131072	69	7	-0.9145
H11	H	0	1	131072	70	1	0.377
H12	H	0	1	131072	71	1	0.377
C21	CT	0	1	131072	72	6	-0.331
H13	HC	0	1	131072	73	1	0.0734
H14	HC	0	1	131072	74	1	0.0734
H15	HC	0	1	131072	75	1	0.0734

Table S23. Average and standard deviation in the χ and θ dihedral angles (deg.) from the last 10 ns of the MD production simulations on duplexes containing COO^- OT-G positioned at G^3 and mismatched against A performed using a 10 Å water box and a non-bonded cut-off of 9 Å.

Conformer	χ	θ
Major groove	210.0 (8.2)	18.1 (6.8)
Wedge	77.4 (13.2)	13.9 (6.6)
Stacked	33.8 (7.8)	352.3 (6.5)

Table S24. Hydrogen-bonding occupancies (%) for simulations on duplexes containing COO^- OT-G positioned at G^3 and mismatched against A from the last 10 ns of the MD production simulation performed using a 10 Å water box and a non-bonded cut-off of 9 Å.

Conformer	Hydrogen bond (OT-G:A)	Occupancy (%)
Major groove	N1(OT-G) – N7(A)	98.2
	O6(OT-G) – N6 (A)	94.6
Wedge	O6(OT-G) – C2 (A)	43.3

Table S25. Average and standard deviation in the χ and θ dihedral angles (deg.) and relative MM-PBSA free energies (kcal mol^{-1}) from 500 ns MD simulations on duplexes containing COO^- OT-G positioned at G^2 and mismatched against T.

Conformer	χ	θ	Relative MM-PBSA free energies
Major groove	204.8 (15.5)	20.2 (6.9)	0.0
Wedge	76.9 (12.2)	16.5 (6.9)	3.0
Stacked	43.2 (20.3)	354.0 (11.7)	22.3

Table S26. Hydrogen-bonding occupancies (%) from 500 ns MD simulations on duplexes containing COO^- OT-G positioned at G^2 and mismatched against T.

Conformer	Hydrogen bond (OT-G:T)	Occupancy (%)
Major groove	N1(OT-G) – O2 (T)	86.1
	O6(OT-G) – N3 (T)	94.1
Wedge	O6(OT-G) – N3 (A)	66.8

References:

(1) Burnouf, D., Koehl, P., and Fuchs, R. (1989) Single adduct mutagenesis: strong effect of the position of a single acetylaminofluorene adduct within a mutation hot spot. *Proc. Natl. Acad. Sci. 86*, 4147-4151.

(2) Millen, A. L., Sharma, P., and Wetmore, S. D. (2012) C8-linked bulky guanosine DNA adducts: experimental and computational insights into adduct conformational preferences and resulting mutagenicity. *Future Med. Chem. 4*, 1981-2007.

(3) Sharma, P., Manderville, R. A., and Wetmore, S. D. (2013) Modeling the conformational preference of the carbon-bonded covalent adduct formed upon exposure of 2′-deoxyguanosine to ochratoxin A. *Chem. Res. Toxicol. 26*, 803-816.

(4) Sharma, P., Manderville, R. A., and Wetmore, S. D. (2014) Structural and energetic characterization of the major DNA adduct formed from the food mutagen ochratoxin A in the *Nar*I hotspot sequence: influence of adduct ionization on the conformational preferences and implications for the NER propensity. *Nucleic Acids Res. 42*, 11831-11845.

(5) Jorgensen, W. L., Chandrasekhar, J., Madura, J. D., Impey, R. W., and Klein, M. L. (1983) Comparison of simple potential functions for simulating liquid water. *J. Chem. Phys. 79*, 926-935.

(6) Case, D. A., Darden, T. A., Cheatham, T. E., Simmerling, C. L., Wang, J., Duke, R. E., Luo, R., Walker, R. C., Zhang, W., Merz, K. M., Roberts, B., Hayik, S., Roitberg, A., Seabra, G., Swails, J., Goetz, A. W., Kolossváry, I., Wong, K. F., Paesani, F., Vanicek, J., Wolf, R. M., Liu, J., Wu, X., Brozell, S. R., Steinbrecher, T., Gohlke, H., Cai, Q., Ye, X., Wang, J., Hsieh, M. J., Cui, G., Roe, D. R., Mathews, D. H., Seetin, M. G., Salomon-Ferrer, R., Sagui, C., Babin, V., Luchko, T., Gusarov, S., Kovalenko, A., and Kollman, P. A. (2012) AMBER 12, University of California, San Francisco.

(7) Pérez, A., Marchán, I., Svozil, D., Sponer, J., Cheatham, T. E., Laughton, C. A., and Orozco, M. (2007) Refinement of the AMBER force field for nucleic acids: improving the description of α/γ conformers. *Biophys. J. 92*, 3817-3829.

(8) Cheatham III, T. E., Cieplak, P., and Kollman, P. A. (1999) A modified version of the Cornell et al. force field with improved sugar pucker phases and helical repeat. *J. Biomol. Struct. Dyn. 16*, 845-862.

(9) Kropachev, K., Ding, S., Terzidis, M. A., Masi, A., Liu, Z., Cai, Y., Kolbanovskiy, M., Chatgilialoglu, C., Broyde, S., and Geacintov, N. E. (2014) Structural basis for the recognition of diastereomeric 5′, 8-cyclo-2′-deoxypurine lesions by the human nucleotide excision repair system. *Nucleic Acids Res. 42*, 5020-5032.

(10) Ding, S., Kropachev, K., Cai, Y., Kolbanovskiy, M., Durandina, S. A., Liu, Z., Shafirovich, V., Broyde, S., and Geacintov, N. E. (2011) Structural, energetic and dynamic properties of guanine (C8)–thymine (N3) cross-links in DNA provide insights on susceptibility to nucleotide excision repair. *Nucleic Acids Res. 40*, 2506-2517.

(11) Kathuria, P., Sharma, P., Manderville, R. A., and Wetmore, S. D. (2017) Molecular modeling of the major DNA adduct formed from the food mutagen ochratoxin A in *Nar*I 2-base deletion duplexes: Impact of sequence context and adduct ionization on conformational preference and mutagenicity. *Chem. Res. Toxicol. 30,* 1582−1591.

(12) Miller III, B. R., McGee Jr, T. D., Swails, J. M., Homeyer, N., Gohlke, H., and Roitberg, A. E. (2012) MMPBSA.py: an efficient program for end-state free energy calculations. *J. Chem. Theory Comput. 8*, 3314-3321.

(13) Witham, A. A., Verwey, A. M., Sproviero, M., Manderville, R. A., Sharma, P., and Wetmore, S. D. (2015) Chlorine functionalization of a model phenolic C8-guanine adduct increases conformational rigidity and blocks extension by a Y-family DNA polymerase. *Chem. Res. Toxicol. 28*, 1346-1356.